Numerical modelling in support of a conceptual model for groundwater flow and geochemical evolution in the southern Outaouais Region, Quebec, Canada

Nelly Montcoudiol[1,2], John Molson[1,*] and Jean-Michel Lemieux[1]

[1]Département de Géologie et de Génie Géologique
Université Laval, Québec, QC, G1V 0A6, Canada
[2]Now at Systems, Power and Energy Research Division, School of Engineering,
University of Glasgow, Glasgow, Scotland, G12 8QQ, UK +44 141 330 2416
Nelly.Montcoudiol@glasgow.ac.uk
* Corresponding author (john.molson@ggl.ulaval.ca)

For the use of the editors

Paper #:

Submitted on:

Accepted on:

Application - Research – Commentary – Book Review:

Abstract

A 2D vertical-section numerical model for groundwater flow and transport of age, tritium and chloride was used to help validate a conceptual model of geochemical evolution within a representative regional-scale hydrogeological system in the Outaouais Region, Quebec, Canada. The flow system includes up to 30 m of Quaternary sediments and marine clays overlying fractured silicate rock of the Canadian Shield. Calibration of the regional flow model using observed piezometric levels and tritium concentrations showed that shallow groundwater flow is dominated by local flow systems limited to 30-40 m depths, 1-5 km

long, and with groundwater residence times of 10-50 years. Intermediate systems, on the order of 5-15 km long, are less extensive than initially thought and are characterized by maximum depths of about 100 m and residence times from 200-6,000 years. A model-calibrated hydraulic conductivity of 8×10^{-5} m/s was required in the upper 50 m of the fractured bedrock. The active flow zone was inferred to extend to depths of about 100-150 m, with any deeper regional flow essentially negligible. Differences between tritium-based ages and simulated mean residence times were attributed to mixing of groundwater in open boreholes. ^{4}He concentrations could be explained by diffusive transport from deeper and older groundwater, exacerbated by sampling. With new insight from the numerical modelling, the conceptual flow model has been updated to now include only a weak component of regional flow combined with significant local and intermediate-scale flow systems connected to the upper fractured bedrock. The simulated flow system is also consistent with the geochemical evolution presented by Montcoudiol et al. (2015), which is dominated by young Ca-HCO_3 –type waters in the unconfined aquifer and by older Cl^- signatures from the remnant Champlain Sea seawater.

KEYWORDS: conceptual model, numerical modelling, tritium transport, groundwater age, Outaouais Region hydrogeology, Canadian Shield

Résumé

Un modèle numérique en 2D vertical d'écoulement et de transport a été utilisé afin d'aider à la validation d'un modèle conceptuel d'évolution géochimique au sein d'un système hydrogéologique régional représentatif de la région de l'Outaouais, Québec, Canada. Le système d'écoulement inclut jusqu'à 30 m de sédiments du Quaternaire et d'argiles marines déposés sur le socle rocheux silicaté et fracturé du Bouclier Canadien. La calibration du

modèle d'écoulement régional basée sur les données de piézométrie et complétées par les teneurs en tritium a montré que les systèmes d'écoulement sont dominés par des systèmes locaux limités aux 30-40 premiers mètres de profondeur et avec des âges de l'eau de 10 à 50 ans. Les systèmes intermédiaires, de l'ordre de 2-5 km de long, sont moins étendus qu'initialement pensé et sont caractérisés par une profondeur d'environ 100 m et des âges entre 200 et 6000 ans. Une conductivité hydraulique élevée (8×10^{-5} m/s, élevée par rapport aux données de terrain), dans les 50 premiers mètres de roc fracturé, a permis d'expliquer la piézométrie et les concentrations en tritium observées. La zone active d'écoulement du modèle calibré a une profondeur d'environ 100-150 m et il n'y a pas d'écoulement au-delà de cette profondeur. Les différences entre le tritium et les temps de résidences moyens modélisés et ceux des échantillons sont dues au mélange dans des puits ouverts aggravés par l'échantillonnage. Les concentrations en ^{4}He sont dues à la diffusion à partir d'eaux souterraines plus âgées, exacerbées par l'échantillonnage. Le modèle conceptuel d'écoulement supporté par le modèle numérique a été actualisé pour maintenant inclure une faible composante d'écoulement régional combinée avec d'importants systèmes d'écoulements locaux et intermédiaires, et connectés à la partie supérieure fracturée du roc. Le système d'écoulement simulé est cohérent avec le modèle d'évolution géochimique présenté par Montcoudiol et al. (2015), dominé par des eaux de type Ca-HCO_3 dans l'aquifère libre et par des signatures de restes de la Mer de Champlain.

MOTS CLÉS : modèle conceptuel, modèle numérique, transport du tritium, âge de l'eau, hydrogéologie de la région de l'Outaouais, bouclier canadien

Introduction

As in many fractured bedrock environments, the Canadian Shield is characterized by a complex geological structure including a variable lithology and mineralogy, as well as by complex faults and fractures (Farvolden et al. 1988). Understanding groundwater flow patterns and geochemical evolution can therefore be challenging in these environments. In the Outaouais Region (southern Quebec, Canada; Figure 1), even the recent geological history is complex and includes invasion and retreat of the Champlain Sea following the last glaciation, which has had lasting effects on the geochemical evolution of groundwater. With increasing stresses on shallow groundwater resources in the region due to a rapidly growing population, water supply is becoming more reliant on the fractured bedrock. Excluding the city of Gatineau, which contains 2/3 of the regional population and which relies mainly on surface water, 91% of the remaining population uses groundwater as their main drinking water supply (Comeau et al. 2013). A better understanding of these resources is important for future development, and for groundwater protection and sustainability.

A conceptual model for groundwater flow and geochemical evolution was recently proposed by Montcoudiol et al. (2015) for the southern Outaouais Region along a 2D cross-section, as shown in Figure 2. As part of their paper, Montcoudiol et al. (2015) used major ion concentrations to identify a chemical zonation of groundwater (Figure 2Figure 2), which was based on a regional-scale study presented in Montcoudiol et al. (2014) and Comeau et al. (2013). The main geochemical processes inferred responsible for this zonation were the dissolution of silicates (mainly anorthite, $CaAl_2Si_2O_8$) in the unconfined (up-gradient) part of the aquifer, mixing with fossil waters from the Champlain Sea invasion and cation exchange in the confined part, as well as mixing between recently-infiltrated and older water

88 in the down-gradient unconfined part (as identified in Figure 2). This hypothesis is tested in
89 the current paper.

90 Remnant seawater from the Champlain Sea invasion was confirmed by field data and
91 evidence of mixing was found between a tritium-rich water component and an older helium-
92 rich component. Montcoudiol et al. (2015) also showed that the hydrochemical system is
93 dynamic and still evolving from induced changes since the last glaciation. Although their
94 conceptual model was developed from detailed field data which yielded much insight into
95 the long-term groundwater flow dynamics and geochemical evolution, several questions
96 remain.

97 One key question concerns the context of local, intermediate and regional flow systems (Tóth
98 1999) in the case of this specific Outaouais flow system and in the more general context of
99 similar settings in southern Quebec and elsewhere within the Canadian Shield. It is still
100 unclear, for example, if a regional flow component exists at the Outaouais site. Groundwater
101 flow simulations by Sykes et al. (2009) in typical Canadian Shield geological settings suggest
102 that, assuming an anisotropy of $K_x/K_z = 0.1$, flow in deep rock is a subdued reflection of the
103 topography rather than being part of a regional component. Gleeson and Manning (2008)
104 also showed that regional flow decreases with lower relief, although this hypothesis has to
105 be tested in the Outaouais case in which the horizontal conductivity is assumed greater than
106 the vertical.

107 In this paper, a 2D vertical-section numerical model for groundwater flow and transport of
108 tritium, chloride and age is developed in order to help validate the conceptual model of
109 Montcoudiol et al. (2015), and to help explain the geochemical evolution of groundwater

110 within the bedrock of the Grenville geologic province (Outaouais Region, Quebec). The flow
111 model was designed in part to help provide insight into the local and intermediate flow
112 systems and to determine their relative importance with respect to groundwater geochemical
113 evolution. The tritium transport model is used to support the flow model calibration.

114 The impact of the Champlain Sea invasion is then assessed by simulating chloride intrusion
115 from the ancient seawater boundary and marine clay into the confined aquifer. Mean
116 groundwater age, including the effect of age dispersion, is also simulated to help interpret
117 geochemical evolution, with simulated ages compared to ages inferred from the observed
118 tritium and ^{14}C data. This is the first detailed quantitative study of relationships between
119 groundwater flow, groundwater age, and geochemical evolution in the context of Quaternary
120 aquifers overlying fractured rock of the Canadian Shield.

121 **Study area and geological history of the region**

122 The study area is located in the southwestern part of the Outaouais region, in southern
123 Québec, Canada (Figure 1). The modelling is applied to a conceptual model proposed by
124 Montcoudiol et al. (2015) which was developed based on interpreting groundwater chemical
125 data along the 2D cross-section identified in Figure 1Figure 1. The cross-section is located
126 along the dominant groundwater flow direction, extending approximately 30 km from the
127 Gatineau Hills in the northeast to the Ottawa River in the southwest, passing through the
128 township of Shawville.

129 **Figure 1 Location of the study area and highlights of the 2D cross-section, including**
130 **the maximum extent of the Champlain Sea (data from Comeau et al.**
131 **(2013)).**

132 The geological history of the region and the resulting distribution of Quaternary deposits
133 within the Outaouais study area were presented by Montcoudiol et al. (2014). A brief review
134 of the geological history is presented herein with a particular focus on the site geology and
135 hydrogeology, and its immediate surroundings.

136 Along the cross-section (Figure 2), the underlying bedrock is part of the Grenville Province
137 of the Canadian Shield, dating from the Proterozoic (Precambrian). The cross-section passes
138 through two principal types of rocks: non-carbonated metamorphic rocks (gneiss and
139 paragneiss) in the northeast and calco-silicate rocks (marble) to the southwest (towards the
140 Ottawa River). The bedrock is characterised by a high degree of stress-induced fracturing in
141 the upper 50-60 m (Sterckx 2013), which has likely produced extensive preferential flow
142 paths.

143 **Figure 2 Conceptual hydrogeological model along the selected 2D cross-section**
144 **perpendicular to the Ottawa River at far right (Montcoudiol et al. 2015)**

145 Unconsolidated deposits left prior to the last glaciation have not been found in the study area,
146 likely due to erosion by the many glacial-deglacial cycles during the Quaternary period
147 (Daigneault et al. 2012). During the last glaciation, abrasion of the bedrock and ice movement
148 deposited a discontinuous layer of till directly overlying the bedrock, while during the last
149 deglaciation, freshwater fluvio-glacial sediments were deposited in the lower valleys. The
150 Ottawa River valley (including lower reaches of secondary river valleys) was then invaded
151 by the Champlain Sea about 12,000 years ago (Parent and Occhietti 1988) which left marine
152 clays on top of the fluvio-glacial sediments (if they had not already been eroded). Due to
153 isostatic rebound, the Champlain Sea progressively left the region about 10,000 years ago,

leaving behind deltaic, littoral and pre-littoral sediments. Along the main rivers, this sequence is buried by ancient and more recent alluvium (Comeau et al. 2013).

Numerical modelling

Simulation approach

A four-step modelling approach is adopted in this study, incorporating groundwater flow, tritium and chloride transport, and mean groundwater age (Figure 3). The first step was to reproduce the current flow conditions, calibrating the model with available hydraulic head data. Since the hydraulic conductivities could not be uniquely calibrated based on observed head data alone (due in part to the sparse available data which were not fully representative of the aquifer conditions), the calibration is improved in Step 2 by simulating the recent tritium distribution throughout the entire aquifer. Using the tritium concentrations in precipitation from the nearby Ottawa meteorological station as a transient surface boundary condition, the theoretical tritium distribution at the sampling date (2012) was compared to the tritium concentrations measured in the groundwater samples and final adjustments made to the hydraulic conductivity field. Step 3 involved simulating the transport and evolution of chloride (as an ideal tracer) following intrusion of water from the Champlain Sea into the aquifer, followed by groundwater freshening after the retreat of the sea, and continuing up to present-day conditions. The aim of this simulation was to explain the current chloride distribution in the aquifer. In Step 4, the steady-state mean groundwater age distribution is simulated under current flow conditions and checked against the tritium and ^{14}C isotope data.

The same 2D vertical domain (including the hydrostratigraphy), which follows the conceptual model of Figure 2, is used for all simulations; only the governing equations and

boundary conditions are changed. An identical spatial discretization was used in all simulations. Considering the regional scale of the model domain (about 32 km) and the lack of data pertaining to the distribution and characteristics of fractures, an equivalent porous medium (EPM) approach was applied in all cases. All simulations were performed with the FLONET/TR2 model. Details on the numerical implementation of the flow and transport equations can be found in Molson and Frind (2014) and are summarized in Appendix I.

Figure 3 Sequential modelling strategy: a) Step 1: steady-state flow model, b) Step 2: calibration of the flow model using tritium, c) Step 3: simulation of chloride transport from the Champlain Sea invasion, and d) Step 4: groundwater age model. For simplicity, the inclined bottom boundary is not shown here. Fixed heads, representing surface water, are shown as small triangles on the water table.

Groundwater flow model

Model domain and flow boundary conditions

The FLONET model domain is 32.5 km long and varies in depth between 550 and 600 m from the ground surface to the bottom boundary. The up-gradient left boundary is located in the Gatineau Hills and corresponds to a surface water divide. The right (down-gradient) boundary is located at the centre of the Ottawa River, which acts as the major discharge zone for the entire Outaouais region. These two boundaries are both set as symmetry (no-flow) boundaries.

The bottom boundary was assumed impermeable (Figure 3a), and assigned a slope similar to the average topographic gradient, varying from -354 to -505 m.a.s.l. A preliminary 10 km deep model (not shown), assuming a uniform hydraulic conductivity of 1×10^{-9} m.s^{-1} below the base of a 100 m deep fractured zone, showed that essentially all groundwater flowed within the shallow Quaternary sediments and upper fractured bedrock zone, with only 0.01%

201 of the total infiltration reaching depths below -350 m.a.s.l. Moreover, at these depths, higher
202 density saline groundwater would further inhibit deeper flow systems (Normani et al. 2009;
203 Sykes et al. 2009).

204 The top boundary of the flow model corresponds to the water table which was initially
205 positioned to correspond with the surface topography, then was allowed to deform during the
206 simulation to its equilibrium position. Topographic elevations (from 268 m.a.s.l. to 72
207 m.a.s.l.) were extracted from a Digital Elevation Model (DEM) with a resolution of 10 m
208 (Comeau et al. 2013). A recharge (Type 2) condition was applied across the top boundary
209 except for surface water bodies which were represented using fixed heads (Type 1) and at
210 the surface of the confining clay layer (treated as a no-flow boundary) (Figure 3a). The
211 applied recharge flux was equivalent to 30% of the total annual precipitation. Indeed, using
212 the model HELP® (Hydrologic Evaluation of Landfill Performance; Schroeder and Ammon
213 (1994)), Comeau et al. (2013) found that in the Outaouais Region, an average of 30% of the
214 precipitation infiltrates as recharge to the aquifers. Observed data from the Shawville
215 meteorological station (station ID 7038040, Environment Canada (2013)) from 1948 to 2012,
216 showed an average annual precipitation rate of about 839 mm/yr., thus a constant recharge
217 rate of 252 mm/yr. was assigned in the model.

218 *Model discretization*

219 The 2D vertical section was discretized with elements every 10 m in the horizontal direction.
220 Vertically, the entire section was divided into 9 hydrostratigraphic layers – the bottom 2
221 layers represent the upper fractured and deeper unfractured bedrock, while the top 7 represent
222 the unconsolidated Quaternary sediments (Table 1). Each hydrostratigraphic layer was
223 discretized vertically into several grid element layers ranging in thickness from 15 m at the

bottom to 0.5 m at the top (Figure 4b and Table 1). The topmost element layer (which follows the water table) is used as a high-K recharge spreading layer that redistributes recharge away from low conductivity zones and avoids the development of ponding conditions (Beckers and Frind 2000). To accommodate the free water table, the grid is allowed to deform vertically (Molson & Frind, 2015). The global mesh is composed of 6514×87 (= 566,718) triangular elements in the horizontal and vertical dimensions, respectively.

Hydraulic properties

Comeau et al. (2013) compiled and validated more than 2,000 hydraulic tests within the top 150 m of unconsolidated sediments and fractured bedrock throughout the Outaouais regional study area (average hydraulic conductivities for each hydrostratigraphic unit are provided in Table 1). Attribution of hydraulic conductivities in the Quaternary sediments is based on the geological cross-section of Figure 2 and data from Comeau et al. (2013) (Figure 4a). Since the hydraulic conductivity of the clay proposed by Comeau et al. (2013) appeared to be too high (2×10^{-7} m.s^{-1}) compared to published values for the Champlain Sea clays (Table 2), a conductivity of 1×10^{-10} m.s^{-1} was applied.

Hydraulic conductivities in the top 50 m of bedrock (assumed highly fractured) and in the underlying 100 m (assumed much less fractured) were assigned based on air-pressure slug tests in 3-m packed intervals (wells CONV-PON and SANDBAY, the latter showing uniform conductivity with depth, Figure 2) and on pumping tests (wells OUT036352 and OUT21341, Figure 2), which yielded hydraulic conductivities between 2×10^{-5} and 3×10^{-8} m.s^{-1} (Figure 4a). These values correspond well to the range for Canadian Shield fractured bedrock observed at the regional scale (Sterckx 2013), where wells have been drilled to a maximum bedrock depth of 150 m. This range of hydraulic conductivities was applied assuming an

247 exponential decrease with depth (Figure 4a), which matches the observed distribution of K
248 values and is commonly observed in crystalline bedrock (Maréchal 1998). Below 150 m, the
249 bedrock is considered to be much less permeable with hydraulic conductivities decreasing
250 from 10^{-10} to 10^{-12} $m.s^{-1}$, again assuming an exponential decrease with depth (Table 1)
251 (Maréchal 1998; Farvolden et al. 1988).

252 Fractured silicate rock is generally anisotropic, characterised by sub-horizontal fractures with
253 ratios of horizontal to vertical hydraulic conductivities of K_x/K_z ranging from 1 to 10
254 (Farvolden et al. 1988; Gleeson 2009). Without any further data on anisotropy at the
255 Outaouais site, a conservative anisotropy factor of 5 ($K_x/K_z = 5$) was applied for the entire
256 bedrock unit. The Quaternary deposits were considered isotropic. This issue is further
257 addressed in the Discussion section.

258 Since measured porosities were not available, values compiled by Fetter (2001) were applied
259 (Table 1Table 1). The clay porosity was later adjusted during calibration to 0.65 which is
260 similar to the mean porosity of similar clays measured by Desaulniers et al. (1989).

261 **Figure 4** **Simulation domain showing: a) Distribution of hydraulic conductivities**
262 **along the 2D cross-section, and b) Selected mesh detail in three areas near**
263 **the fluvio-glacial sediment-clay interface. The vertical bars represent the**
264 **wells shown in Figure 2. Asterisks identify wells where hydraulic**
265 **conductivities (shown in bold) were calculated from hydraulic testing. For**
266 **clarity, the full depth of 550 to 600 m is not shown. K distribution is shown**
267 **for Step 3b (following seawater retreat); Step 3a (during seawater**
268 **intrusion) was identical but had low-K marine clay instead of the high K**
269 **alluvium near the far right boundary.**

Chloride transport model: Two-step modelling strategy

Chloride evolution in the 2D section (Figure 3c) was simulated in two sub-steps, invoking a change in boundary conditions between flooding by saltwater of the Champlain Sea (Step 3a; applying a constant seawater elevation over the affected area) and following its retreat (Step 3b; applying surface recharge), and accounting for the replacement of marine clay by river alluvium sediments near the far right boundary. Only the hydraulic conductivity distribution and boundary conditions were changed between sub-steps, and the simulated chloride concentrations at the end of Step 3a were used as the initial condition for Step 3b.

Step 3a: Champlain Sea invasion

Step 3a was simulated to represent the approximately 1200-year period of saltwater invasion from the Champlain Sea (Catto et al. 1981). The clay layer left by the Champlain Sea was assumed to have been rapidly deposited, and its pore water was assumed initially saturated with seawater (Desaulniers et al. (1989), Figure 3c). During the Champlain Sea invasion (Step 3a), alluvium from the Ottawa River was not yet present, thus the hydraulic conductivity in this area (which was needed for Step 3b) was assigned the hydraulic conductivity of clay, which is considered justified as marine clay lenses have been discovered in boreholes drilled along the Ottawa River (MDDEFP 2012). An initial normalized chloride concentration of $C/C_0 = 1$ was imposed as the initial condition in all clay units. The rest of the domain had an initial concentration of 0 (Figure 3Figure 3c).

The transport model in this study did not include density-driven flow since a) horizontal flow gradients dominate throughout the system, especially following retreat of the Champlain Sea,

292 and b) water from the Champlain Sea, being far from the ocean and at this late stage of
293 inundation, was considered to be diluted marine water with a significant proportion of ice-
294 melt (fresh) water. Analyses of clay pore water by Catto et al. (1981), for example, in the
295 area of Chalk River (~ 100 km upstream of Shawville on the Ottawa River) revealed
296 Champlain Sea salinities between 12 and 16 $g.l^{-1}$, similar to the maximum concentration
297 measured by Cloutier et al. (2010) in marine clays from the Montreal area, about 200 km
298 downstream. Others have found similar salinities, including Desaulniers et al. (1989) in
299 marine clays near Montreal, and Quigley et al. (1983) in clays between Ottawa and Montreal.
300 It is likely that the salinity was higher in the deep water-body of the central Champlain Sea
301 but became more diluted during latter stages of the invasion and along its long arms which
302 extended inland (Torrance 1988).

303 Deep, brackish formation water was also not included in the model. The depth of the interface
304 between fresh water and brackish groundwater in Canadian Shield areas has been observed
305 to vary from 200 m (Frape and Fritz 1987) to 650 m (Frape et al. 1984). Salinity in the
306 Canadian Shield generally does not exceed 1,000 $mg.l^{-1}$ at depths less than 500 m (Gascoyne
307 and Kamineni 1994; Farvolden et al. 1988). Furthermore, at the nearby Chalk River nuclear
308 facility, where extensive investigations have been carried out for sighting nuclear fuel
309 repositories, groundwater TDS content does not exceed 700 $mg.l^{-1}$ at a depth of 400 m. An
310 initial concentration of 0 was therefore assigned throughout the bedrock where the average
311 TDS content would only be about 5% of the Champlain Sea concentration.

312 The extent of the top seawater boundary condition was based on Barnett (1988) who found
313 evidence for Champlain Sea elevations of 170 m.a.s.l. in the Renfrew area, which faces
314 Shawville on the opposite bank of the Ottawa River. This elevation also corresponds to the

maximum elevation of the clay layer on the 2D cross-section. Along the same boundary surface, a Cauchy (Type 3) transport boundary condition (Molson et al. 2014) was set with a normalized chloride concentration of $C/C_0 = 1$ (Figure 3Figure 3d). In the valleys within the northern (up-gradient) part of the cross-section, some clay deposits were also found, suggesting that the Champlain Sea probably reached even higher elevations but likely lasted a shorter time and thus would have had less impact on the hydrochemistry. We also assumed that the transitional period from one hydraulic regime to another was short and the flow system responded immediately to these changes.

The duration of marine transgression varied within the basin, depending on the distance from the mouth of the St. Lawrence River. Our study area is located in an extreme north-western arm of the Champlain Sea, where the ice cover lasted longer, and where seawater invasion occurred relatively later (Catto et al. 1981). Two events of marine transgression have been identified in the nearby region of Renfrew. The first event lasted less than 200 years, between 12,150 and 12,000 years BP after which the Champlain Sea retreated in step with a new advance of the ice sheet for about 1,000 years. The second phase of the Champlain Sea lasted about 1,200 years, from the ice retreat 11,400 years BP to the withdrawal of the sea at about 10,200 years BP due to isostatic rebound (Catto et al. 1981). For modelling purposes, the first phase is considered negligible and only the second phase is simulated, representing 1,200 years of seawater intrusion (Figure 3Figure 3d).

Step 3b: Champlain Sea retreat

Similar to the assumption of rapid marine transgression, seawater retreat and flow system response is also assumed to be rapid. After the retreat of the Champlain Sea about 10,200 years ago (Catto et al. 1982), the flow systems (including boundary conditions) were assumed

to be similar to those of today, even though the Ottawa River valley has had its current shape for only about the last 8,000 years (Catto et al. 1982; Teller 1990). Isostatic rebound is not taken into account by the model although groundwater systems are dynamic and are still evolving as a result of the Laurentide Ice Sheet melting (Sykes et al. 2009; Lemieux et al. 2008). In Step 3b, following seawater retreat, the clay layer within 2.5 km of the Ottawa river, which was initially present in Step 3a, is replaced by permeable river alluvium (K= 5×10^{-4} m/s).

In Step 3b, a Cauchy condition is again applied at the top boundary, but with a chloride concentration set to 0 representing low chloride content in rainwater. The initial condition in the domain corresponds to the final chloride distribution from the previous (Step 3a) model. The Step 3b chloride transport model is run for 10,200 years (Figure 3Figure 3d).

Groundwater age model: Initial and boundary conditions

The TR2 transport module of FLONET/TR2 was subsequently applied to simulate mean steady-state groundwater residence times (advective-dispersive ages), according to Equation 4. In the age simulation, all nodes corresponding to recharge at the top surface are assigned as Type 1 fixed age boundaries (A = 0 yrs) while all other boundaries are assigned zero age-gradient conditions with the initial age set at 0 throughout the domain (Figure 3Figure 3d). All other parameters (dispersivities, diffusion coefficient, retardation factor and decay constant) remain the same as for the transport of chloride.

Modelling results

Calibration of the flow model: hydraulic heads and tritium

Calibration of the hydraulic conductivity in the flow model was first completed using only the hydraulic head data (Figure 5Figure 5). The observed head dataset includes 27 wells within 1 km of the 2D cross-section which were validated at the regional scale (for errors, anomalous data etc.) by Comeau et al. (2013). Most measurements (15/27) were taken in wells located in the confined bedrock aquifer. The few measurements (7/27) taken from the unconfined bedrock aquifer are located in the valleys of the higher topographic regions. The remaining head measurements (5/27) were taken in the unconfined aquifer near the Ottawa River.

As pointed out by Ophori (1999), calibration to hydraulic heads alone is non-unique based on uncertain combinations of recharge and hydraulic conductivity (K). To improve the calibration, the flow model was also checked by comparing simulated and observed tritium distributions. The initial simulated tritium concentrations based on the head-calibrated flow model showed a relatively poor fit with essentially no tritium predicted for the shallow bedrock. A final re-calibration of K was therefore performed with insights from the observed tritium distribution, whose concentrations are more sensitive to changes in the hydraulic parameters, especially the hydraulic conductivity of the shallow bedrock. This additional step also helped improve the calibration to the hydraulic heads, the final hydraulic conductivity values being significantly higher than the initial estimate (Table 1Table 1).

Tritium concentrations were available for 12 wells (Montcoudiol et al. 2015) along the 2D cross-section (Figure 2Figure 2). Although the decrease in tritium activity due to migration

379 time within the unsaturated zone is not taken into account in the model, the water table is
380 relatively shallow in most parts of the aquifer (except in the topographic highs) thus travel
381 times through the unsaturated zone would be short relative to the total residence time and this
382 limitation would therefore not significantly affect the results.

383 The initial conditions for the transient tritium simulation from 1953-2012 were based on a
384 simulated steady-state tritium distribution assuming the current-condition flow field, and a
385 constant Type-1 concentration of 15 TU's across the watertable (Clark et al. 1997). Tritium
386 concentrations measured on a monthly basis at the Ottawa meteorological station (WMO
387 code 7162800, IAEA/WMO (2011)) were then used as the top boundary condition from 1953
388 to 2012 (Figure 3Figure 3b). A few missing data points were replaced by the average value
389 between the closest measurement times. The series ends in 2007. From this last measurement
390 to the sampling date, an average value of 15 TU was applied, similar to the background value
391 (which also corresponds to the average value of the two final years of measurements).

392 The flow model calibration to hydraulic heads (Figure 5Figure 5) showed that irrespective of
393 the transverse distance of the observation wells from the 2D cross-section, the deviation from
394 the 1:1 best-fit line was minimal which confirms that the 2D cross-section indeed closely
395 follows a regional flow line and thus a 2D vertical model is considered an acceptable
396 simplification. The root mean squared error (RMSE) is less than 5 m, with calculated heads
397 on average 1.2 m greater than those measured (Figure 5Figure 5). In the unconfined aquifer,
398 the water table is below ground surface (up to 60 m deep) whereas the confined aquifer is
399 partly under artesian conditions (up to 3.7 m above ground). Artesian conditions were
400 confirmed by a flowing well at one of the sampled wells.

Figure 5 Calibration results: simulated vs. observed heads

Test simulations showed that when the shallow bedrock *K* was too low, the simulated tritium would remain only in the Quaternary sediments. In the final calibrated model, with a higher hydraulic conductivity of 8×10^{-5} $m.s^{-1}$ in the shallow bedrock, a more reasonable RMSE value of 6.1 TU was obtained. However, the simulated concentrations were still almost systematically under-estimated compared to tritium contents measured in the field (Table 3).

Since the model did not simulate the decay of tritium due to increased travel time through the unsaturated zone, over-estimated tritium concentrations were expected. Different hypotheses can be made to explain the discrepancies. First, a greater proportion of water sampled from the bedrock wells would likely have originated from fracture zones, whereas the model-based concentrations in the bedrock wells were averaged over the length of the open borehole. The equivalent porous medium approach used in the model would also tend to decrease the tritium compared to tritium migration through discrete fractures. Furthermore, in the 5 bedrock wells cased through the overlying Quaternary deposits (other than those through marine clay), leakage from shallow (younger) groundwater might be expected since the shallow bedrock is fractured. For wells in the Quaternary deposits, the location of the well screen was not known, but for simplicity, the well was considered screened over the bottom 5 metres.

Simulated flow systems

The simulated steady-state groundwater flow system and advective (particle-track) travel times (residence times from recharge to discharge) along selected streamlines are shown in Figure 6Figure 6. Flow system depths and the extent of intermediate flow systems are

423 controlled by the hydraulic K distribution, topography and by surface water bodies which act
424 as discharge zones (Figure 6Figure 6a). Local flow systems (on horizontal scales of ~1-5 km)
425 are located in the first 50 metres below ground surface. All intermediate systems (~5-15 km)
426 reach the base of the model but flow rates are essentially negligible at these depths (evident
427 from the exponential decrease in streamfunction contour levels with depth). The simulation
428 showed no evidence of regional groundwater flow at scales greater than 15 km.

429 Due to the rapid decrease of hydraulic conductivity in the bedrock at depths greater than 150-
430 200 m, maximum particle-tracking based groundwater residence times are on the order of
431 hundreds of thousands of years. Detail shown in Figure 6Figure 6b reveals primarily short
432 residence times (< 100 years) in the first tens of metres of depth, within the Quaternary
433 sediments. Residence times are longer for groundwater infiltrating from high-elevation rock
434 outcrop areas, with flow paths controlled by the layer geometry. Groundwater discharging to
435 the central discharge zones of large surface water bodies has originated from deeper flow
436 paths and has longer mean residence times (up to 18,000 yrs) compared to groundwater
437 discharging into small rivers, especially below Lake Johnson (at km 1-2). In the confined
438 aquifer (Figure 6Figure 6c), groundwater flows most rapidly in the upper fractured part of
439 the bedrock, with groundwater residence times of less than 100 years.

440 **Figure 6 Simulated flow system showing: a) steady-state flow lines, and b) detail of**
441 **flow systems in the unconfined aquifer, including total residence times from**
442 **recharge to discharge, shown on corresponding streamlines (streamlines**
443 **are identified by streamfunction contours in $m^2.s^{-1}$, e.g. 1E-06; residence**
444 **times are shown in years (bold text), ex. 3 yrs). For clarity, the full depth of**
445 **550 to 600 m is not shown.**
446

447 In recharge and discharge zones, the decreasing hydraulic conductivity with depth has
448 induced significant variations in the hydraulic heads. Below discharge areas, hydraulic heads

449 are relatively constant in the first 200 m and increase between 0.5 and 1 m over the remaining
450 model depth (with a vertical hydraulic gradient ∇h of 1.4 to 2.9×10^{-3} m/m, Figure A1Figure
451 A1a and Figure A1e in Appendix II) whereas they decrease by 6 m over the same depths
452 below recharge zones ($\nabla h = -1.1\times10^{-2}$ m/m, Figure A1Figure A1b). In the clay layer
453 overlying the up-gradient part of the confined aquifer (Figure A1Figure A1c), hydraulic
454 heads increase with depth in the clay and in the upper part of the bedrock, and decrease with
455 depth into the deeper bedrock (-2×10^{-3} m/m). In the down-gradient part of the confined
456 aquifer, hydraulic heads are higher in the deep bedrock (Figure A1Figure A1d) than in the
457 fractured bedrock. Artesian conditions therefore prevail in the up-gradient part of the
458 confined aquifer while fluxes are downward further down-gradient.

459 Analysis of vertical flux variations with depth (not shown) reveals that 99% of the total
460 recharge remains within the first 100-200 m of the watertable, (depending on the position
461 along the cross-section), which corresponds to the Quaternary deposits and the shallow
462 fractured bedrock ($K = 8\times10^{-5}$ m.s^{-1}, Table 1Table 1). In recharge areas where hydraulic
463 gradients are high but hydraulic conductivities are low (ex. thin layers of Quaternary deposits
464 or outcropping bedrock), groundwater fluxes remain low. Maximum fluxes are found in the
465 fluvio-glacial sediments. Although the depth of the active flow zone is conditioned by the
466 thickness of the most permeable layer of bedrock, these results are in agreement with
467 observations made in similar settings of the Canadian Shield (Gascoyne 2004; Manning and
468 Caine 2007; Farvolden et al. 1988).

469

470 ***Simulated chloride distribution***

471 The simulated chloride distribution at the end of the Champlain Sea invasion 10,200 years
472 ago (end of Step 3a) as well as its current expected distribution (end of Step 3b), is shown in
473 Figure 7Figure 7a and Figure 7c, respectively. Figure 7b represents an intermediate time 800
474 years after the retreat of the Champlain Sea.

475 Due to the constant sea level of 170 m elevation imposed in Step 3a, velocities in the upper
476 fractured part of the bedrock are 100 times less than under current conditions and mean
477 residence times are longer. The flow patterns are also different from the current conditions.
478 Most water which has infiltrated up-gradient of the clay layer discharges just before the
479 aquifer becomes confined. Groundwater flowing within the confined fractured bedrock
480 aquifer recharges from further up-gradient. Two distinct discharge areas can be identified:
481 one where the till currently outcrops (ca. km 30) and one at the far down-gradient end of the
482 2D cross-section. At the end of the Champlain Sea invasion (Figure 7Figure 7a), chloride
483 from the marine clay begins diffusing downwards into the shallow fractured bedrock aquifer
484 which is recharged by chloride-free rainwater. Once in the bedrock, chloride is transported
485 rapidly down-gradient. A gap in the simulated chloride plume is seen at km 30, where a
486 preferential discharge zone has formed due to more permeable overburden.

487 Chloride concentrations in the clay are still elevated 800 years following seawater retreat
488 (Figure 7Figure 7b), whereas all chloride in the aquifer has been flushed away by freshwater
489 recharging in the unconfined part. Velocities below the centre of the Ottawa River are slower
490 and chloride is still found in significant concentrations.

The chloride distribution 10,200 years following seawater retreat (Figure 7Figure 7c) shows that most of the initial chloride in the bedrock aquifer has been flushed away (where concentrations are less than 1000 $mg.l^{-1}$), with most of the residual chloride still found in the marine clay. Maximum chloride concentrations in the clay remain about 11,000 $mg.l^{-1}$, similar to the original assumed seawater concentrations. This behaviour is consistent with a theoretical case described by Atteia et al. (2005) who show diffusion from a seawater-saturated aquitard into a confined fresh water aquifer. The results are also generally consistent with the observed chloride concentrations in most of the sampled wells and with investigations in similar marine clays presented, for example, by Cloutier et al. (2010) and Desaulniers et al. (1989). Some differences were observed, however, in concentrations below 1000 $mg.l^{-1}$. Sample OUT036356 in the confined aquifer, for example, had a Na-Cl water type (Figure 2Figure 2) and the highest chloride concentration (around 350 $mg.l^{-1}$), whereas the corresponding simulated concentration was much lower (6 $mg.l^{-1}$). Calculated concentrations for wells OUT026131 and OUT022292 are 10 times lower than those measured in the corresponding samples whereas they are in the same order of magnitude for the SANDBAY well (15 $mg.l^{-1}$ for calculated and observed values) and for well OUT21341 (15 $mg.l^{-1}$ calculated vs. 12 $mg.l^{-1}$ observed). Differences could be simply due to heterogeneities in the fractured bedrock, which would also explain why the observed concentration in sample OUT036356 was higher compared to the others, if this sample was located in a less permeable zone. In the field, chloride concentrations above the drinking water standard of 250 $mg.l^{-1}$ are currently found only in the clay layer. Concentrations are below this limit in the aquifer where chloride has been flushed by fresh water.

Figure 7 Simulated chloride distribution from t = 0, representing the start of the Champlain Sea invasion, showing a) Step 3a: Simulated Cl after 1,200 years

of seawater invasion (about 10,200 years ago); b) Intermediate step at t = 2,000 years (800 years after seawater retreat) and c) Step 3b: current conditions 11,400 years after the start of sea invasion (10,200 years since seawater retreat). Selected streamlines are also shown (with 10× less groundwater flux in each successively deeper streamtube. Points 2, 4 and 5 are located on the same streamline which passes through the confined aquifer. Vertical exaggeration is 45×. For clarity, only the local area impacted by the seawater is shown. Concentrations are based on a maximum seawater concentration of 15 g.l^{-1} (Catto et al. 1981). Blanked areas represent concentrations < 250 mg.l^{-1} (drinking water standard in Canada). See Appendix II (Figure A2) for concentration breakthrough curves at selected points 1-6.

Simulated chloride concentrations over time are shown in Figure A2Figure A2a and Figure A2b of Appendix II at three different sites in the overburden (points 1 and 3 in the clay and 5 in the alluvium) and three in the confined fractured bedrock aquifer (points 2, 4 and 6) (see locations inFigure 7). During invasion of the Champlain Sea, the clay remains saturated in chloride (points 1 & 3) while chloride in the fractured bedrock aquifer at point 4 gradually increases. Chloride concentrations in the up- and down-gradient parts of the bedrock aquifer (points 2 & 6) remain near zero.

Following seawater retreat, the breakthrough curves in the clay follow a slow diffusion-controlled decline, while points 4 and 6 in the fractured bedrock (now under the new hydraulic regime with higher flow gradients) are rapidly flushed by freshwater (Figure A2Figure A2a). Below the Ottawa River, the initial chloride in the alluvium (point 5) is also quickly removed. Under the higher flow gradients, chloride migrating through the upper fractured bedrock had also penetrated into the deeper unfractured bedrock, reaching a depth of 100 m at km 31, about 200-300 years after the Champlain Sea retreat. Thus, low-concentration chloride signals are seen at the base of the bedrock aquifer at points 4 and 6

542 (Figure A2Figure A2b), which are only slowly decreasing because of low velocities below
543 the Ottawa River and slow back-diffusion from the deeper rock.

544 Over the 10,200 year simulation time after seawater retreat, chloride has also diffused
545 upwards at the surface of the clay over a thickness of about 5 m (Fig. A2c of Appendix II),
546 resulting in similar profiles to those described by O'Shaughnessy and Garga (1994).
547 Diffusion towards the bottom of the clay layer (Figure A2Figure A2c) is similar to
548 observations by Torrance (1979) for other sites in the Ottawa region. Artesian conditions can
549 also play a role in the leaching of marine clays (Torrance 1979; Rankka et al. 2004).

550

551 ***Age distribution***

552 The age model was run for 100,000 years which was sufficient to reach steady state within
553 the first 200 m of depth (Figure 8Figure 8a). Mean residence times in the Quaternary deposits
554 were less than 100 years and were less than 10 years in the Ottawa River alluvium. Age
555 contours are controlled by the flow system and by dispersion, with generally increasing ages
556 with depth. An important exception is below the clay layer where younger, more recently
557 recharged water can be found in the confined aquifer below the older water trapped in the
558 clay. At depths greater than about 150 m, groundwater is more than 50,000 years old due to
559 very low-flow conditions and limited mixing. Typical age profiles at different locations in
560 the aquifer can be found in Appendix II (Figure A3Figure A3). Under large surface-water
561 bodies, for example under Lake Johnson at km 2, (Figure A3Figure A3a and Figure 8Figure
562 8b) or below the Ottawa River (Figure A3Figure A3d and Figure 8c), ages rapidly increase
563 with depth due to the low hydraulic gradients and low groundwater velocities. Ages greater

than 1,000 years are evident in the unfractured bedrock with low hydraulic conductivities (with $K \leq 10^{-7}$ m.s^{-1}). Marine clays are characterised by ages greater than 20,000 years whereas groundwater in the underlying higher-K fractured bedrock layer is younger due to rapid displacement of groundwater from the nearest recharge zone (Figure A3Figure A3c and Figure 8c). In the unconfined aquifer, the maximum advective-dispersive ages are similar to the advective-based residence times (Figure 6Figure 6) whereas in the confined aquifer, mixing of older water into younger water results in much higher advective-dispersive ages.

Figure 8 Simulated steady-state mean groundwater ages, showing a) the 2D cross-section to a depth of -100 m.a.s.l., b) age detail in the upgradient part of the unconfined aquifer, and c) age detail in the confined aquifer with overburden and rock interfaces shown for reference (dashed lines).

Discussion and validation of the conceptual model

Model Sensitivity

Anisotropy

Little information is available on the bedrock anisotropy in this study area, although fractures are known to exist (as shown by the packer test results in well CONV-PON, Figure 4**Erreur ! Source du renvoi introuvable.**). In another part of the Grenville Province of the Canadian Shield, Lavigne et al. (2010) considered the Precambrian basement as isotropic at depths below 200 m, although this was not based on literature or field data. At the Whiteshell Research Area (Superior Province of the Canadian Shield, southern Manitoba, Canada), Ophori et al. (1996) and Sykes et al. (2009) accounted for vertical fractures by applying an anisotropy factor $K_x/K_z = 0.1$ to a depth of 300 m. Below this depth, the bedrock was considered isotropic. Additional simulations of the Outaouais flow system (not shown) showed that anisotropy has relatively little impact on the distribution of local and

588 intermediate flow systems since the bulk hydraulic conductivity decreases so rapidly with
589 depth.

590 *Hydraulic and transport properties*

591 The simulated tritium distribution was much more sensitive to the hydraulic conductivity of
592 the bedrock than to the Quaternary deposits, which are on average only about 20 m thick with
593 relatively high hydraulic conductivities, allowing rapid migration of tritium toward the
594 bottom of these layers. Transport through the fractured bedrock was thus the main control on
595 tritium behaviour, because of the bedrock's relatively lower K, and because of the longer
596 spatial scales for the local flow systems which were on the order of 1 to 5 km. This behaviour
597 also reflects the hydraulic link between the Quaternary sediments and the fractured bedrock.

598 The sensitivity of tritium transport to changes in recharge rates was also tested (using 10, 20
599 and 35% of total precipitation). Simulated tritium concentrations showed only minor changes
600 within the range of uncertainty in recharge compared to changes in the bedrock hydraulic
601 conductivities. A lower longitudinal dispersivity of α_{LH} = 10 m (compared to the base case
602 α_{LH} = 20 m) showed a slightly less extended but more concentrated tritium plume (especially
603 in zones of high velocities). Excessively high dispersivities tended to homogenise and
604 decrease the tritium concentrations, which also did not reflect the observations.

605 *Chloride transport scenarios*

606 The chloride transport simulation assumed a single 1,200-year Champlain Sea invasion, and
607 neglected an inferred initial 200-year invasion. Within a reasonable uncertainty of +/- 200
608 years, errors in assuming a shorter 1,200-year duration would appear to have a limited effect
609 on the final results since the simulated chloride plume had almost reached steady state within
610 1,200 years following seawater invasion while most chloride had been flushed away within

611 a few hundred years after its retreat. Thus, a possible 200-year invasion episode followed by
612 1,000 years of ice advance before the major invasion of 1,200 years most likely would not
613 have changed the final result.

614 The impact of the maximum estimated elevation reached by the Champlain Sea (170 m.a.s.l.),
615 which corresponded to the maximum elevation of the clay layer, was also of interest, in
616 particular since some marine clays had been found at higher elevations of around 180 m.a.s.l.,
617 notably in the unconfined part of the aquifer (at km 14-15). In a subsequent simulation (not
618 shown), a higher fixed head of 180 m was applied in all areas less than 180 m in elevation,
619 again with a fixed concentration of $C/C_0 = 1$ allowing intrusion of salt water. Assuming the
620 same invasion duration of 1,200 years, chloride was again rapidly flushed away after the
621 Champlain Sea retreat, indicating results were not sensitive to the intrusion duration.

622 The progressive sedimentation of marine clays and sea level rise were not tested in this study
623 but they would be expected to have some impact on the flow patterns and on the chloride
624 plume development. It would be of interest to model more realistic scenarios to justify the
625 simplifications and compare simulated current chloride plumes.

626 The modelling results suggest that seawater intrusion into the deeper unfractured bedrock did
627 not occur during the Champlain Sea invasion (Figure 7Figure 7a). Following seawater retreat,
628 the simulated chloride plume does penetrate the upper part of the less fractured bedrock but
629 remains for less than 1,000 years (Figure 7Figure 7b) as it is slowly replaced by freshwater.
630 At the end of the simulation, the chloride concentrations in this part of the bedrock aquifer
631 have decreased to about 10-15 mg/l.

632 A similar conceptual model was proposed by Aquilina et al. (2015) in which saline
633 groundwater in a basement aquifer in France was quickly replaced by mobile freshwater but
634 remained in the deeper bedrock. In our case, the study area is located in an arm of the
635 Champlain Sea where the seawater was diluted (15,000 mg/l) and the invasion episode was
636 short. Intrusion of seawater into the deeper bedrock was likely limited at the Outaouais site
637 and became slowly diluted after the Champlain Sea retreat. However, no samples from the
638 deeper bedrock in this area are available to validate this hypothesis.

639 ***Comparison of ages***

640 Most of the bedrock boreholes pass through different groundwater age layers (Figure 9Figure
641 9). As explained in Montcoudiol et al. (2015), the groundwater samples show evidence of
642 both low mean residence times (where tritium was detected) and higher mean residence times
643 (accumulation of ^{4}He). For the four boreholes sampled for noble gases (Montcoudiol et al.
644 2015), it appears that the average (relatively young) age is not consistent with the high
645 concentrations of helium 4 but rather reflects the maximum age of the groundwater
646 component flowing through the open borehole, which seems to be a better indicator. For
647 example, CONV-PON has the lowest concentration of helium 4 and has the smallest
648 simulated age range (from 11 to 23 years along the open borehole, Figure 9Figure 9c). On
649 the other hand, OUT036356 does not show evidence of tritium and has calculated ages
650 varying from 580 to 900 years (Figure 9Figure 9f). Finally, wells OUT036357 and
651 OUT021341 present the highest ^{4}He concentrations as well as the largest simulated age
652 range, from 6 to 1,430 and from 1 to 1,530 years, respectively (Figure 9Figure 9b and Figure
653 9Figure 9i), with detected concentrations of tritium.

Observed ^{14}C measurements for each well are also given in Figure 9Figure 9. The modelling results show that the ^{14}C concentrations cannot be used for assessing mean groundwater residence times as they are not correlated to simulated ages. They rather reflect processes occurring in the unsaturated and saturated zones, as discussed in Montcoudiol et al. (2015). Only the ^{14}C age calculated for sample OUT036356 (the only sample to have undergone some decay, see Montcoudiol et al. (2015)) can be compared with the modelling results. The simulated age is lower than the estimated ^{14}C age and lower than the age suggested by the chemical data. As mentioned before, chloride simulations suggested that sample OUT036356 comes from a well which is probably located within a less permeable zone where ages are higher than those calculated by the model.

Figure 9 Simulated advective-dispersive groundwater age and tritium profiles for selected wells: a) OUT036352, b) OUT036357, c) CONV-PON, d) OUT036358, e) OUT036353, f) OUT036356, g) SANDBAY, h) OUT036351 and i) OUT021341. The simulated ages and tritium concentrations represent average values based on the open borehole length for bedrock wells and the entire well length for wells in Quaternary sediments for which the location of the screen is unknown.

Note that simulated groundwater ages greater than the depositional age of their host formations (ex. ages of 20,000 years for the marine clays) are not inconsistent, this simply reflects the theoretical mean steady-state age which would be reached (ex. in the future) under uniform conditions.

Validation of the conceptual model

The updated conceptual model with the interpreted flow systems and groundwater residence times is shown in Figure 10. A major change to the original conceptual model was the removal of a regional flow component. In general, local flow systems had already been well

679 identified, but intermediate flow systems are now thought to be laterally less extensive but
680 also deeper, extending the modelling results from Sykes et al. (2009) and Ophori et al. (1996)
681 to different set of conditions in the Canadian Shield, while regional-scale flow remains
682 negligible. Topography and surface water bodies also exercise a more important control than
683 initially thought as most areas of local topographic minima (corresponding to streams, lakes
684 and rivers) are locations of strongly focussed discharge.

685 In this new conceptual model, vertical flow gradients in the confined aquifer have now been
686 clarified. Specifically, the confined aquifer is now divided into two parts, with the up-
687 gradient area (from km 23 to 24) characterized by upward vertical flow gradients (referred
688 to previously as flowing artesian) whereas the down-gradient part has downward vertical
689 flow gradients. These findings need to be verified against more detailed and reliable data
690 (only one artesian well was found in this part of the confined aquifer). Regardless of the flow
691 gradient directions, groundwater flow is very slow in the clay where chloride transport is
692 dominated by downward diffusion into the fractured bedrock, where it becomes diluted due
693 to rapidly flowing freshwater. Some upward diffusion towards surface fresh water is also
694 suggested.

695 The simulated lateral extent of intermediate flow systems, which has been reduced in the new
696 conceptual model, has an impact on how the chemistry data should be interpreted. All
697 samples were originally believed to have been taken along a flow line from an intermediate
698 flow system extending along most of the 2D cross-section and were assumed to represent the
699 geochemical evolution of groundwater. Although this is true in the confined part, all samples
700 taken in the up-gradient unconfined bedrock are now presumed to belong to different flow
701 systems, reflecting their own geochemical evolution depending on their mean residence

times. Samples OUT036358 and OUT036353, located in highly conductive fluvio-glacial sediments, show significant rock-water interactions compared to samples from the unconfined bedrock (Montcoudiol et al. 2015). While these sediments result from glacial erosion and have similar mineral chemistry to the bedrock, the higher mineralization of the samples could be explained by their proximity to the underlying marble bedrock (Montcoudiol et al. 2015).

Local flow systems are characterized by very short residence times of less than 50 years, which explains the occurrence of tritium in most samples from the unconfined aquifer. Fast simulated flow conditions in the unconfined bedrock aquifer are consistent with the observed chemical composition of groundwater, which shows limited interaction between groundwater and rock. The high chloride concentration in sample OUT036356 cannot be accurately simulated and likely reflects unresolved heterogeneities and less permeable zones, also suggested by the low ^{14}C activity. Except for this sample, ^{14}C contents cannot be interpreted because in addition to radioactive decay, they are adversely affected by chemical reactions occurring in the unsaturated and saturated zones (Montcoudiol et al. 2015) which are not taken into account in the model. Finally, old groundwater is found at intermediate depths (about 150-200 m) from which diffusion of ^{4}He could explain the high concentrations of this element measured in some samples (Andrews 1987).

Figure 10 Final revised conceptual model, showing flow directions and total residence times from recharge to discharge zones along selected conceptual flow lines

722

723 ***Modelling approach and limitations***

724 The two-dimensional models developed here are relatively simple with respect to the
725 complexity of the real system and the chronology of past events. For example, groundwater
726 ages were simulated over a 100,000 year period assuming no changes in flow conditions.
727 While model sensitivity tests showed that the simplifications applied to represent the
728 Champlain Sea invasion (sea level rise, rate of clay sedimentation and uplift) did not have a
729 significant impact on the final results representing current conditions, the system response
730 time to these major system changes was not tested. Groundwater ages for example, especially
731 in the Quaternary sediments and fractured bedrock where residence times are short, would
732 likely be affected by uplift, which is a slow process occurring over 10,000 years. The rate of
733 clay sedimentation and sea level rise would also likely have some impact on the chloride and
734 age distribution, since the flow velocities become negligible under hydrostatic conditions
735 below the seawater. However, the speed at which the confined aquifer recovered from the
736 retreat of the Champlain Sea, from one extreme to the other, is probably the main factor
737 controlling the extent of the current chloride plume.

738 As expected, the distribution of the hydraulic conductivities at depth exerts an important
739 control on the flow systems, affecting both the extent and depth of the tritium and chloride
740 plumes as well as on the age distribution. Transport modelling thus appears to be a good
741 means to improve the flow model calibration. The tritium simulation showed that the
742 hydraulic conductivities had to be high in the upper part of the bedrock to allow sufficient
743 penetration of the tritium and to explain the occurrence of tritium concentrations well above
744 the detection limits in the unconfined bedrock wells. The estimated horizontal hydraulic

745 conductivity in the fractured bedrock is only a bulk EPM value as flow would be faster in
746 fractures while negligible in the matrix. The simplified (EPM) modelling approach could
747 therefore explain why calculated tritium concentrations were generally less than measured in
748 the field.

749 Evidence of such highly-conductive bedrock zones was demonstrated by Sterckx (2013) in
750 his analysis of aquifer transmissivities calculated from hydraulic tests. Furthermore,
751 hydraulic packer tests carried out in two wells along the cross-section (CONV-PON and
752 SANDBAY) responded completely differently, with the SANDBAY well being tight all
753 along the open borehole, whereas well CONV-PON was characterised by a highly-
754 conductive zone at depths between 20 and 25 m. Packer test results suggested hydraulic
755 conductivities on the order of 10^{-5} $m.s^{-1}$ at this location which was similar to the model-
756 calibrated value.

757 Most of the wells are located in areas where the flow is assumed sub-horizontal and mixing
758 would occur as a result of sampling in open boreholes. Areas of natural flow mixing also
759 occur near the discharge zones, as in bedrock well OUT021341 close to the Ottawa River.
760 Generally, vertical profiles, from ground surface to the bottom of the wells, show tritium
761 concentrations close to present atmospheric levels near the surface. Since atmospheric tritium
762 has been almost constant over the last approximately 10 years, tritium which has infiltrated
763 into the first few metres during this period has already been partly degraded and
764 concentrations are thus less than the current atmospheric tritium levels. Concentrations then
765 increase with depth, corresponding to what is left of the historic tritium peak, and are still
766 higher than the current levels. At deeper depths, tritium is absent and is representative of

767 levels which had recharged before the bomb testing peak and which have been decaying for
768 several decades.

769

Conclusions and perspectives

Four sequential numerical modelling approaches (for groundwater flow, and transport of tritium, chloride and age) were developed to support a 2D vertical plane conceptual hydrogeochemical model along a 32 km flow path representative of the western Outaouais area, Quebec, Canada. Calibration of the flow model was augmented using tritium which appeared to be most sensitive to the hydraulic conductivity of the upper fractured bedrock, which was calibrated to 8×10^{-5} m.s^{-1}. This is relatively high for bedrock but consistent with discrete hydraulic conductivities measured using packer tests and specific capacity tests in other regional wells, and supports the conclusion of Sterckx (2013), that the upper part of the bedrock is densely fractured.

The flow simulation showed negligible regional flow at scales > 15-30 km. The simulated intermediate systems, on scales of 5-15 km, are likely less laterally extensive than proposed in the original conceptual model. Therefore, only those water samples taken just up-gradient of the confined aquifer and those from the confined aquifer likely lie along the same flow path. Samples from different locations within the unconfined bedrock aquifer likely belong to different intermediate flow systems. Their relatively similar chemistry, which suggests limited water-rock contact time (Montcoudiol et al. 2015), is the result of similar mean residence times on the order of 100's of years within different intermediate flow systems.

Local flow system depths predicted by the model appear limited to the first 40 metres, and mainly lie within the Quaternary sediment layers and the first tens of metres of bedrock in outcropping areas. These local flow systems are characterised in the model by scales of 1-5 km and by residence times of a few tens of years or less, explaining the occurrence of tritium.

792 The active flow zone appears to extend only into the first 100-150 m, with almost stagnant
793 conditions below this depth (residence times > 10^5 yrs). Old groundwater is often found at
794 relatively shallow depths (excluding recharge and discharge zones) from which diffusion of
795 ^{4}He can explain the high concentrations found in the samples.

796 The simulations support the conceptual model that the Champlain Sea invasion caused
797 diluted seawater to migrate into the hydraulically connected Quaternary deposits and
798 fractured upper bedrock aquifer system, but due to short mean residence times of less than
799 1,000 years, all chloride has since been flushed from the active flow system. Current residual
800 chloride concentrations likely result from slow diffusion out of the clay layer and subsequent
801 mixing with up-gradient groundwater. High chloride concentrations in sample OUT036356
802 are probably indicative of heterogeneities and less conductive areas as commonly found in
803 fractured bedrock but which are not resolved in the current model.

804 Relatively short residence times and a predominance of local flow systems suggest a
805 relatively vulnerable aquifer system, even within the shallow confined fractured bedrock
806 where in direct contact with the unconfined aquifer. Relatively rapid infiltration from surface
807 contaminants, for example agricultural fertilizers, could therefore be a risk to local water
808 supply wells. Nevertheless, water supplies within the conductive Quaternary aquifers have
809 good potential for providing additional high quality potable water as outlined in Montcoudiol
810 et al. (2014). Although the apparently highly fractured shallow bedrock appears sufficient for
811 meeting local household water supplies, the storage volumes would still be limited,
812 restricting more intense development of the resource.

The numerical flow and transport modelling has provided much insight into the hydrogeological system, however improvements could be made through the collection of additional data, specifically in the clays and within the fractured bedrock. Tracer tests would be very useful to independently constrain flow velocities. A more complete validation of the conceptual model would also require geochemical modelling which at this scale would need additional simplifications. For example, one approach could focus on silicate weathering along a flow line or on cation exchange in the confined aquifer. These approaches will be considered in future work.

Acknowledgements

This project was funded primarily by the Quebec Ministry of Sustainable Development, Environment, and the Fight against Climate Change (MDDELCC), with contributions from the following Regional Partners: l'Agence de Traitement de l'Information Numérique de l'Outaouais (L'ATINO), WESA Enviro-Eau, Regional County Municipalities (Collines de l'Outaouais, Vallée de la Gatineau, Pontiac and Papineau), the City of Gatineau, Regional Watershed Organisations (ABV des 7, COBALI and OBV-RPNS), and the Regional Council for Environment and Sustainable Development in Outaouais (CREDDO). We also acknowledge research support from the Natural Sciences and Engineering Research Council of Canada (NSERC) and from a Canada Research Chair in Quantitative Hydrogeology of Fractured Porous Media held by the second author. We thank P. Therrien of Université Laval who provided invaluable computer technical support. Finally, we would like to thank CWRJ Co-editor Jim Buttle, Clément Roques (ETH Zurich), and an anonymous reviewer for their helpful comments.

835

References

Andrews, J. 1987. Noble gases in groundwaters from crystalline rocks. In *Saline water and gases in crystalline rocks*, ed. P. Fritz and S. K. Frape. St John's, Newfoundland, Canada: Geological Association of Canada.

Aquilina, L., V. Vergnaud-Ayraud, A. A. Les Landes, H. Pauwels, P. Davy, E. Pételet-Giraud, T. Labasque, C. Roques, E. Chatton, O. Bour, S. Ben Maamar, A. Dufresne, M. Khaska, C. L. G. La Salle, and F. Barbecot. 2015. Impact of climate changes during the last 5 million years on groundwater in basement aquifers. *Scientific Reports* 5: 14132.

Atteia, O., L. Andre, A. Dupuy, and M. Franceschi. 2005. Contributions of diffusion, dissolution, ion exchange, and leakage from low-permeability layers to confined aquifers. *Water Resources Research* 41(9): W09412.

Barnett, P. 1988. History of the northwestern arm of the Champlain Sea. In *The Late Quaternary Development of the Champlain Sea Basin*, ed. N. R. Gadd. 25-36. St John's, Newfoundland, Canada: Geological Association of Canada.

Beckers, J., and E. O. Frind. 2000. Simulating groundwater flow and runoff for the Oro Moraine aquifer system. Part I. Model formulation and conceptual analysis. *Journal of Hydrology* 229(3–4): 265-80.

Bester, M. L., E. O. Frind, J. W. Molson, and D. L. Rudolph. 2006. Numerical Investigation of Road Salt Impact on an Urban Wellfield. *Ground Water* 44(2): 165-75.

856 Catto, N. R., R. J. Patterson, and W. A. Gorman. 1982. The late Quaternary geology of the
857 Chalk River region, Ontario and Quebec. *Canadian Journal of Earth Sciences* 19(6):
858 1218-31.

859 ———. 1981. Late Quaternary marine sediments at Chalk River, Ontario. *Canadian Journal*
860 *of Earth Sciences* 18(8): 1261-67.

861 Clark, I., and P. Fritz. 1997. *Environmental Isotopes in Hydrogeology*. Boca Raton, Florida,
862 USA: CRC-Press/Lewis Publishers.

863 Cloutier, V., R. Lefebvre, M. M. Savard, and R. Therrien. 2010. Desalination of a
864 sedimentary rock aquifer system invaded by Pleistocene Champlain Sea water and
865 processes controlling groundwater geochemistry. [In English]. *Environmental Earth*
866 *Sciences* 59(5): 977-94.

867 Comeau, G., M.-C. Talbot Poulin, Y. Tremblay, S. Ayotte, J. Molson, J.-M. Lemieux, N.
868 Montcoudiol, R. Therrien, R. Fortier, P. Therrien, and G. Fabien-Ouellet. 2013.
869 *Projet d'acquistion de connaissances sur les eaux souterraines en Outaouais -*
870 *Rapport final [Groundwater characterisation program in Outaouais - Final report]*.
871 Département de géologie et de génie géologique, Université Laval. 148 pp.

872 Daigneault, R.-A., M. Roy, M. Lamothe, P.-M. Godbout, S. Milette, É. Leduc, N. Horth, M.
873 Dubois-Verret, M.-A. Hurtubise, and O. Lamarche. 2012. *Rapport sur les travaux de*
874 *cartographie des formations superficielles réalisés dans la portion est du territoire*
875 *municipalisé de l'Outaouais en 2011-2012 [Report on the mapping of superficial*
876 *formations in the eastern portion of the Outaouais Region in 2011-2012]*. Montréal,

877 Canada: Département des sciences de la Terre et de l'Atmosphère et Département de
878 géographie, Université du Québec à Montréal

879 Desaulniers, D. E., and J. A. Cherry. 1989. Origin and movement of groundwater and major
880 ions in a thick deposit of Champlain Sea clay near Montréal. *Canadian Geotechnical*
881 *Journal* 26(1): 80-89.

882 Duhaime, F., E. M. Benabdallah, and R. P. Chapuis. 2013. The Lachenaie clay deposit: some
883 geochemical and geotechnical properties in relation to the salt-leaching process.
884 *Canadian Geotechnical Journal* 50(3): 311-25.

885 Environment Canada. 2013. *Historical climate data.* www.climate.weatheroffice.gc.ca
886 (accessed October, 2013).

887 Farvolden, R., O. Pfannkuch, R. Pearson, and P. Fritz. 1988. Region 12, Precambrian Shield.
888 In *The Geology of North America.* 101-14: The Geological Society of America.

889 Fetter, C. W. 2001. *Applied Hydrogeology*. 4th ed. Upper Saddle River, New Jersey, USA:
890 Prentice Hall.

891 Frape, S., and P. Fritz. 1987. Geochemical trends for groundwaters from the Canadian Shield.
892 In *Saline water and gases in crystalline rocks*, ed. P. Fritz and S. K. Frape. 19-38. St
893 John's, Newfoundland, Canada: Geological Association of Canada.

894 Frape, S. K., P. Fritz, and R. H. McNutt. 1984. Water-rock interaction and chemistry of
895 groundwaters from the Canadian Shield. *Geochimica et Cosmochimica Acta* 48(8):
896 1617-27.

897 Garga, V. K., and V. O'Shaughnessy. 1994. The hydrogeological and contaminant-transport
898 properties of fractured Champlain Sea clay in Eastern Ontario. Part 2. Contaminant
899 transport. *Canadian Geotechnical Journal* 31(6): 902-15.

900 Gascoyne, M. 2004. Hydrogeochemistry, groundwater ages and sources of salts in a granitic
901 batholith on the Canadian Shield, southeastern Manitoba. *Applied Geochemistry*
902 19(4): 519-60.

903 Gascoyne, M., and D. C. Kamineni. 1994. The hydrogeochemistry of fractured plutonic rocks
904 in the Canadian Shield. [In English]. *Applied Hydrogeology* 2(2): 43-49.

905 Gleeson, T. 2009. *Groundwater recharge, flow and discharge in a large crystalline*
906 *watershed*. PhD thesis, Queen's University.

907 Gleeson, T., and A. H. Manning. 2008. Regional groundwater flow in mountainous terrain:
908 three-dimensional simulations of topographic and hydrogeologic controls. *Water*
909 *Resour. Res.* 44(10): W10403.

910 IAEA/WMO. 2011. *Global Network of Isotopes in Precipitation. The GNIP Database.*
911 http://www.iaea.org/water (accessed September, 2011).

912 Lapierre, C., S. Leroueil, and J. Locat. 1990. Mercury intrusion and permeability of
913 Louiseville clay. *Canadian Geotechnical Journal* 27(6): 761-73.

914 Lavigne, M.-A., M. Nastev, and R. Lefebvre. 2010. Numerical Simulation of Groundwater
915 Flow in the Chateauguay River Aquifers. *Canadian Water Resources Journal / Revue*
916 *canadienne des ressources hydriques* 35(4): 469-86.

917 Lemieux, J. M., E. A. Sudicky, W. R. Peltier, and L. Tarasov. 2008. Simulating the impact
918 of glaciations on continental groundwater flow systems: 2. Model application to the
919 Wisconsinian glaciation over the Canadian landscape. *Journal of Geophysical*
920 *Research: Earth Surface* 113(F3): F03018.

921 Leroueil, S., M. Diene, F. Tavenas, M. Kabbaj, and P. La Rochelle. 1988. Direct
922 determination of permeability of clay under embankment. *Journal of Geotechnical*
923 *Engineering* 114(6): 645-57.

924 Leroueil, S., K. Hamouche, F. Ravenasi, M. Boudali, J. Locat, D. Virely, T. Tan, K. Phoon,
925 and D. Hight. 2003. Geotechnical characterization and properties of a sensitive clay
926 from Quebec. In *Characterization and engineering properties of natural soils*, ed. T.
927 S. Tan, K. Phoon, D. Hight and S. Leroueil. 363-94. The Netherlands: A.A. Belkema.

928 Lichtner, P. C., S. Kelkar, and B. Robinson. 2002. New form of dispersion tensor for
929 axisymmetric porous media with implementation in particle tracking. *Water*
930 *Resources Research* 38(8): 21-1-21-16.

931 Manning, A. H., and J. S. Caine. 2007. Groundwater noble gas, age, and temperature
932 signatures in an Alpine watershed: Valuable tools in conceptual model development.
933 *Water Resources Research* 43(4): W04404.

934 Maréchal, J.-C. 1998. *Les circulations d'eau dans les massifs cristallins alpins et leurs*
935 *relations avec les ouvrages souterrains [Flow patterns in alpine cristalline massifs*
936 *and their intereactions with underground facilities]*. PhD thesis, Département de
937 Génie Civil, EPFL.

938 Marques, M. E. S., S. Leroueil, and M. d. S. Soares de Almeida. 2004. Viscous behaviour of
939 St-Roch-de-l'Achigan clay, Quebec. *Canadian Geotechnical Journal* 41(1): 25-38.

940 MDDEFP. 2012. *Système d'information hydrogéologique [Hydrogeological Information*
941 *System]*. http://www.mddelcc.gouv.qc.ca/eau/souterraines/sih/ (accessed November,
942 2014).

943 Molson, J. W., and E. O. Frind. 2014. *User guide version 3.0 for Flonet/TR2 - A two-*
944 *dimensional simulator for groundwater flownets, contaminant transport and*
945 *residence time*. Université Laval & University of Waterloo. 55 pp.

946 Montcoudiol, N., J. W. Molson, and J. M. Lemieux. 2014. Groundwater geochmistry of the
947 Outaouais Region (Québec, Canada): a regional-scale study. *Hydrogeology Journal*
948 23(2): 377-96.

949 Montcoudiol, N., J. W. Molson, J. M. Lemieux, and V. Cloutier. 2015. A conceptual model
950 for groundwater flow and geochemical evolution in the southern Outaouais region,
951 Québec, Canada. *Applied Geochemistry* 58: 62-77.

952 Normani, S., J. Sykes, and Y. Yin. 2009. Regional-scale paleoclimate influences on a
953 proposed Deep Geologic Repository in Canada for low and intermediate level waste.
954 In Proceedings of the 3rd CANUS Rock Mechanics Symposium, Toronto, Canada,
955 May 11-13, 2009.

956 O'Shaughnessy, V., and V. K. Garga. 1994. The hydrogeological and contaminant-transport
957 properties of fractured Champlain Sea clay in Eastern Ontario. Part 1.
958 Hydrogeological properties. *Canadian Geotechnical Journal* 31(6): 885-901.

959 Ophori, D. U. 1999. Constraining permeabilities in a large-scale groundwater system through
960 model calibration. *Journal of Hydrology* 224(1–2): 1-20.

961 Ophori, D. U., A. Brown, T. Chan, C. Davison, M. Gascoyne, N. Scheier, F. Stanchell, and
962 D. Stevenson. 1996. *Revised model of regional groundwater flow in the Whiteshell*
963 *Research Area*. Atomic Energy of Canada Ltd., Pinawa, MB (Canada). Whiteshell
964 Labs

965 Parent, M., and S. Occhietti. 1988. Late Wisconsinan deglaciation and Champlain Sea
966 invasion in the St. Lawrence Valley, Québec. *Géographie physique et Quaternaire*
967 42(3): 215-46.

968 Quigley, R. M., Q. H. J. Gwyn, O. L. White, R. K. Rowe, J. E. Haynes, and A. Bohdanowicz.
969 1983. Leda clay from deep boreholes at Hawkesbury, Ontario. Part I: Geology and
970 geotechnique. *Canadian Geotechnical Journal* 20(2): 288-98.

971 Rankka, K., Y. Andersson-Sköld, C. Hultén, R. Larsson, V. Leroux, and T. Dahlin. 2004.
972 *Quick clay in Sweden*. Statens Geotekniska Institut (Swedish Geotechnical Institute),
973 Linköping, Sweden

974 Schroeder, P. R., and D. C. Ammon. 1994. *The hydrologic evaluation of landfill performance*
975 *(HELP) model: User's guide for version 3*. Risk Reduction Engineering Laboratory,
976 Office of Research and Development, US Environmental Protection Agency

977 Sterckx, A. 2013. *Étude des facteurs influençant le rendement des puits d'alimentation de*
978 *particuliers qui exploitent le roc fracturé en Outaouais, Québec, Canada [Study of*
979 *the factors impacting on the productivity of individual wells in fractured bedrock from*

the Outaouais Region, Québec, Canada]. Master thesis, Département de Géologie et Génie Géologique, Université Laval.

Sykes, J. F., S. D. Normani, M. R. Jensen, and E. A. Sudicky. 2009. Regional-scale groundwater flow in a Canadian Shield setting. *Canadian Geotechnical Journal* 46(7): 813-27.

Tavenas, F., P. Jean, P. Leblond, and S. Leroueil. 1983. The permeability of natural soft clays. Part II: Permeability characteristics. *Canadian Geotechnical Journal* 20(4): 645-60.

Tecplot Inc. 2014. *Tecplot 360 EX 2014, User's Manual*. Bellevue, WA, USA: Tecplot Inc. 488 pp.

Teller, J. T. 1990. Volume and routing of late-glacial runoff from the southern Laurentide Ice Sheet. *Quaternary Research* 34(1): 12-23.

Torrance, J. K. 1988. Mineralogy, pore-water chemistry, and geotechnical behaviour of Champlain Sea and related sediments. In *The Late Quaternary Development of the Champlain Sea Basin*, ed. N. R. Gadd. 259-75. St John's, Newfoundland, Canada: Geological Association of Canada.

———. 1979. Post-depositional changes in the pore-water chemistry of the sensitive marine clays of the Ottawa area, eastern Canada. *Engineering Geology* 14(2–3): 135-47.

Tóth, J. 1999. Groundwater as a geologic agent: an overview of the causes, processes, and manifestations. *Hydrogeology Journal* 7(1): 1-14.

1001

1002 **Appendix I: Governing equations of the numerical models**

1003

1004 ***Groundwater flow***

1005 The flow system representing the conceptual model was simulated using the FLONET/TR2
1006 model (Molson et al. 2014) which uses the dual formulation for flow in terms of hydraulic
1007 potentials Φ [L] and stream functions ψ [$L^2.T^{-1}$], assuming 2D steady-state, isothermal and
1008 uniform density conditions, as defined by Equation 1 and Equation 2, respectively:

1009

1010 $$\frac{\partial}{\partial x}\left(K_{xx}\frac{\partial \phi}{\partial x}\right)+\frac{\partial}{\partial y}\left(K_{yy}\frac{\partial \phi}{\partial y}\right)=0 \quad (1)$$

1011

1012 $$\frac{\partial}{\partial x}\left(\frac{1}{K_{yy}}\frac{\partial \psi}{\partial x}\right)+\frac{\partial}{\partial y}\left(\frac{1}{K_{xx}}\frac{\partial \psi}{\partial y}\right)=0 \quad (2)$$

1013

1014 where x and y are the horizontal and vertical coordinate directions, respectively [L], and K_{xx}
1015 and K_{yy} are the principal components of the hydraulic conductivity tensor [$L.T^{-1}$].

1016 Element-based groundwater velocities for the transport simulations are calculated in
1017 FLONET/TR2 based on the simulated stream functions. These velocities are used to calculate
1018 advective groundwater ages based on particle tracking using a 4th-order Runge-Kutta
1019 integration scheme within Tecplot (©Tecplot Inc. (2014)). A full advective-dispersive age
1020 transport simulation is presented later in the paper. The flow field is assumed at steady state
1021 for all simulations.

Tritium and chloride

Tritium and chloride transport is simulated using the TR2 module within FLONET/TR2 which solves the 2D advective-dispersive mass transport equation (Equation 3):

$$\frac{\partial}{\partial x_i}\left(\frac{D_{ij}}{R}\frac{\partial c}{\partial x_j}\right) - \frac{v_i}{R}\frac{\partial c}{\partial x_i} - \lambda t = \frac{\partial c}{\partial t} \quad (1)$$

where D_{ij} is the hydrodynamic dispersion tensor [$L^2.T^{-1}$], R is the retardation factor [-], c is the tritium or chloride concentration [$M.L^{-3}$], x_i are the spatial coordinates [L], v_i is the average linear flow velocity [$L.T^{-1}$], λ is the first-order decay rate [T^{-1}] and t is the time [T].

For tritium, a retardation factor of R = 1 and a linear decay rate of $\lambda = 1.53\times10^{-4}$ d^{-1} was applied, which corresponds to a half-life of 12.43 years (Clark and Fritz 1997). For chloride, which is non-reactive, λ = 0 and R = 1. The effective molecular diffusion coefficient for tritium was 1×10^{-10} $m^2.s^{-1}$, and for chloride was 2×10^{-10} $m^2.s^{-1}$ (Desaulniers and Cherry 1989; Quigley et al. 1983).

The dispersion tensor D_{ij} in Equation 3 is defined using the 4-component dispersivity formulation of Lichtner et al. (2002), which uses two principal longitudinal dispersivities (α_{LH}, α_{LV}) and two principal transverse dispersivities (α_{TH}, α_{TV}), for the horizontal and vertical directions, respectively. In all transport simulations, the longitudinal horizontal dispersivity for the domain (α_{LH} = 20 m) was estimated using the relationships developed by Gelhar et al. (1992). The longitudinal vertical dispersivity (α_{LV}) was set at 2 m, (10× less than α_{LH}) while the two transverse dispersivities were set at 0.01 m (same order of magnitude as

applied at similar scales by Bester et al. (2006). See Molson et al. (2014) for the full dispersion tensor formulation, including diffusion.

The tritium and chloride transport simulations assume steady-state flow conditions and dilute water. Density effects are not considered. The time step was 10 days which meets the Courant stability criterion.

Groundwater mean age

Advective-dispersive mean groundwater ages were computed to complement the advective ages as the former include full mixing between different age groundwaters, and are therefore more realistic than advective travel times. A similar equation to Equation 3 is solved for mean groundwater age (Equation 4):

$$\frac{\partial}{\partial x_i}\left(D_{ij} \frac{\partial A}{\partial x_j} \right) - v_i \frac{\partial A}{\partial x_i} + 1 = 0 \qquad (2)$$

where A is groundwater age (T) relative to a recharge age of 0 days, and where the +1 term represents a growth of age at a rate of 1 day/day. The dispersion tensor and dispersivities are defined identically as in the tritium and chloride simulations. A molecular diffusion coefficient of 1×10^{-10} $m^2.s^{-1}$ was assumed. The approach accounts for advective-dispersive age mixing along and across flow lines.

Appendix II: Additional figures

Figure A1 **Simulated hydraulic head profiles within the 2D cross-section in different hydrogeological settings: a) discharge zone under Lake Johnson, b) recharge zone, c) artesian conditions, d) non-artesian conditions in the confined aquifer, and e) discharge zone under the Ottawa River**

Figure A2 **Simulated chloride variations over time at different points in the model showing response and decay since flooding (t = 0) and retreat (t = 1200 years) of the Champlain Sea: a) Chloride response within the overburden (points 1 and 3 in the marine clay, point 5 in the alluvium), b) Response within the bedrock (points 2, 4 and 5 are located along the same flow line), and c) Chloride variations over depth at 1,200 and 11,400 years at x = 27,000 m (passing through point 2 and 5). See Figure 7 for point locations.**

Figure A3 **Simulated age profiles along the 2D cross-section in different hydrogeological settings: a) in a discharge zone under Lake Johnson, b) in a recharge zone, c) in the confined aquifer, and d) in the discharge zone below the Ottawa River**

Table 1 Description of the hydrostratigraphic units and their hydraulic properties

Stratigraphic unit	Vertical discretization (# of grid layers)	Hydraulic conductivity ($m.s^{-1}$)*	Porosity (-)
RSL (Recharge Spreading Layer)	1	$1x10^{-5}$	0.30
Alluvium	2	$1x10^{-4}$ [$5x10^{-4}$]	0.35
Deltaic sediments	4	$1x10^{-4}$ [$2x10^{-4}$]	0.30
Littoral sediments	1	$3x10^{-4}$	0.35
Marine clays	4	$1x10^{-10}$	0.50 [0.65]
Fluvio-glacial sediments	4	$3x10^{-4}$ [$1x10^{-4}$]	0.25
Till	1	$8x10^{-5}$	0.15
Shallow bedrock (fractured)	8	$1x10^{-6}$ [$8x10^{-5}$] (top 50 m)	0.03
Deep bedrock (less fractured and/or unfractured)	42	$1x10^{-7}$ (40-50 m thick)	0.02
		$1x10^{-8}$ (50-60 m thick)	0.01
		$1x10^{-10}$ (60-70 m thick)	0.01
		$1x10^{-12}$ (to bottom)	0.01
Transport parameters: α_{LH} = 20 m; α_{LV} = 2 m and $\alpha_{TH} = \alpha_{TV}$ = 0.01 m			

* Initial estimated K values are from Comeau et al. (2013)

[-]: final calibrated values of hydraulic conductivities and porosity

Table 2 Literature review of measured hydraulic conductivities and porosities of Champlain Sea clay deposits

Reference	Hydraulic conductivity ($m.s^{-1}$)	Porosity [-]
Tavenas et al. (1983)	$1\times10^{-11} – 1\times10^{-10}$	
Leroueil et al. (1988)	$1\times10^{-9} – 5\times10^{-9}$	
Desaulniers et al. (1989)	$7.5\times10^{-11} – 4.9\times10^{-10}$	0.64
Lapierre et al. (1990)	$\sim 1\times10^{-9}$	
O'Shaughnessy et al. (1994) and Garga and O'Shaughnessy (1994)	$8\times10^{-10} – 2\times10^{-9}$	0.5
Leroueil et al. (2003)	$\sim 1\times10^{-9}$	
Marques et al. (2004)	$\sim 1\times10^{-9}$	
Duhaime et al. (2013)	$3\times10^{-11} – 5\times10^{-9}$	

Table 3 Comparison between observed and simulated tritium concentrations

Well ID	Measured tritium (TU)	Simulated tritium (TU)
OUT036352	16.9	9.9
OUT036357	14.9	12.4
CONV-PON	18.8	12.5
OUT036358*	20.7	9.3
OUT036353*	15.1	9.2
OUT036356	<0.8	11.8
SANDBAY	10.9	11.8
OUT021341	9.8	11.5
OUT036351*	17.5	12.2

* Wells in Quaternary sediments with no information on the screen location, for which simulated concentrations assume a screened interval 5 m long at the bottom of the well.

List of figures

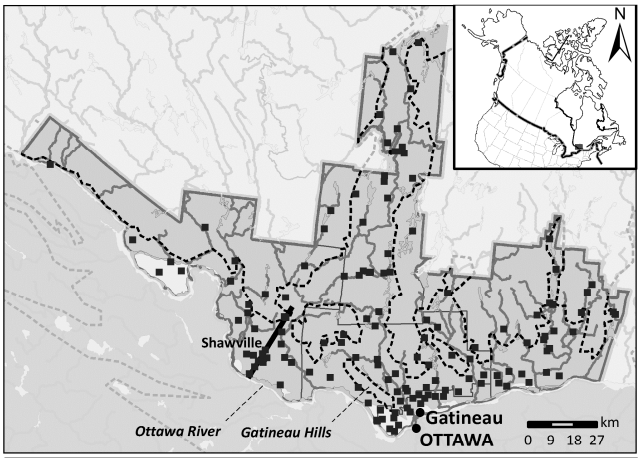

Legend

- Regional County Municipalities
- Lake
- Streams & rivers

Municipalities of interest

- < 5000 inhab.
- > 100000 inhab.

- Limit of the study area
- Max. extension of Champlain Sea
- Groundwater sample
- 2D cross-section

Geologic provinces

- Grenville Province
- St. Lawrence Platform

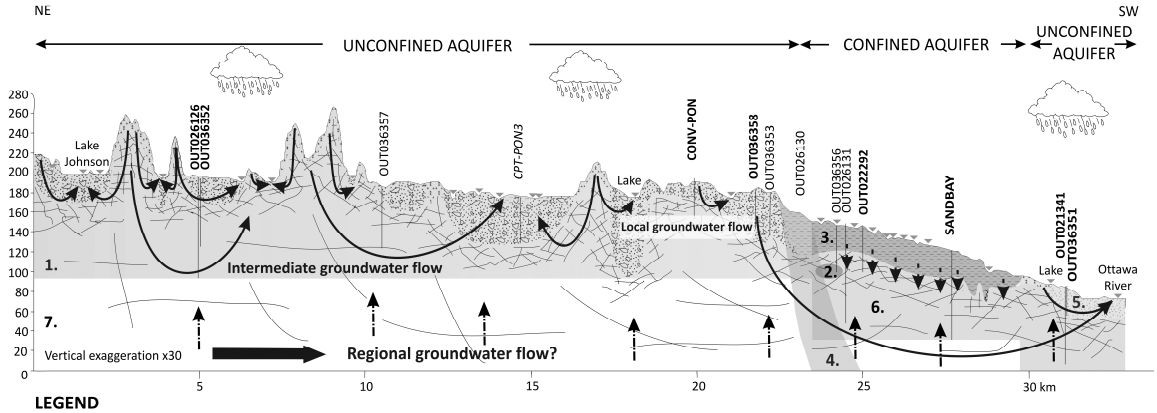

LEGEND

Geology

Quaternary deposits

- Alluvial deposits (sand)
- Marine clay
- Surface water
- Sand & gravel
- Till

Bedrock

- Fractured Canadian Shield

Fluxes

- Groundwater flow
- Diffusive flux of NaCl
- Diffusive flux of ^4He

Well identification

Well ID: well on the flow line

Well ID: well a bit offset from the flow line

Well ID: well offset from the flow line (chemistry considered as representative of the geologic unit)

Geochemical zones

1. **Ca-HCO_3 water type**
   Increase of Ca^{2+}, HCO_3^- and TDS concentrations along the flow path (silicate weathering)
   Na-Cl water type
2. Remnant Champlain Sea water (stagnant zone)
3. Probably mixed with Ca-HCO_3 water type at the top of the clay layer (Na-HCO_3)
4. **Transition zone**
5. **Ca-HCO_3 water type**
   Discharge zone characterised by mixing with Na-HCO_3 water type
6. **Na-HCO_3 water type**
   Na^+/Ca^{2+} cation exchange (Na-Cl water type flushed away by Ca-HCO_3 water type)
7. **No available chemical data**
   Most likely Ca-HCO_3 and Na-HCO_3 up and down-gradient of the transition zone

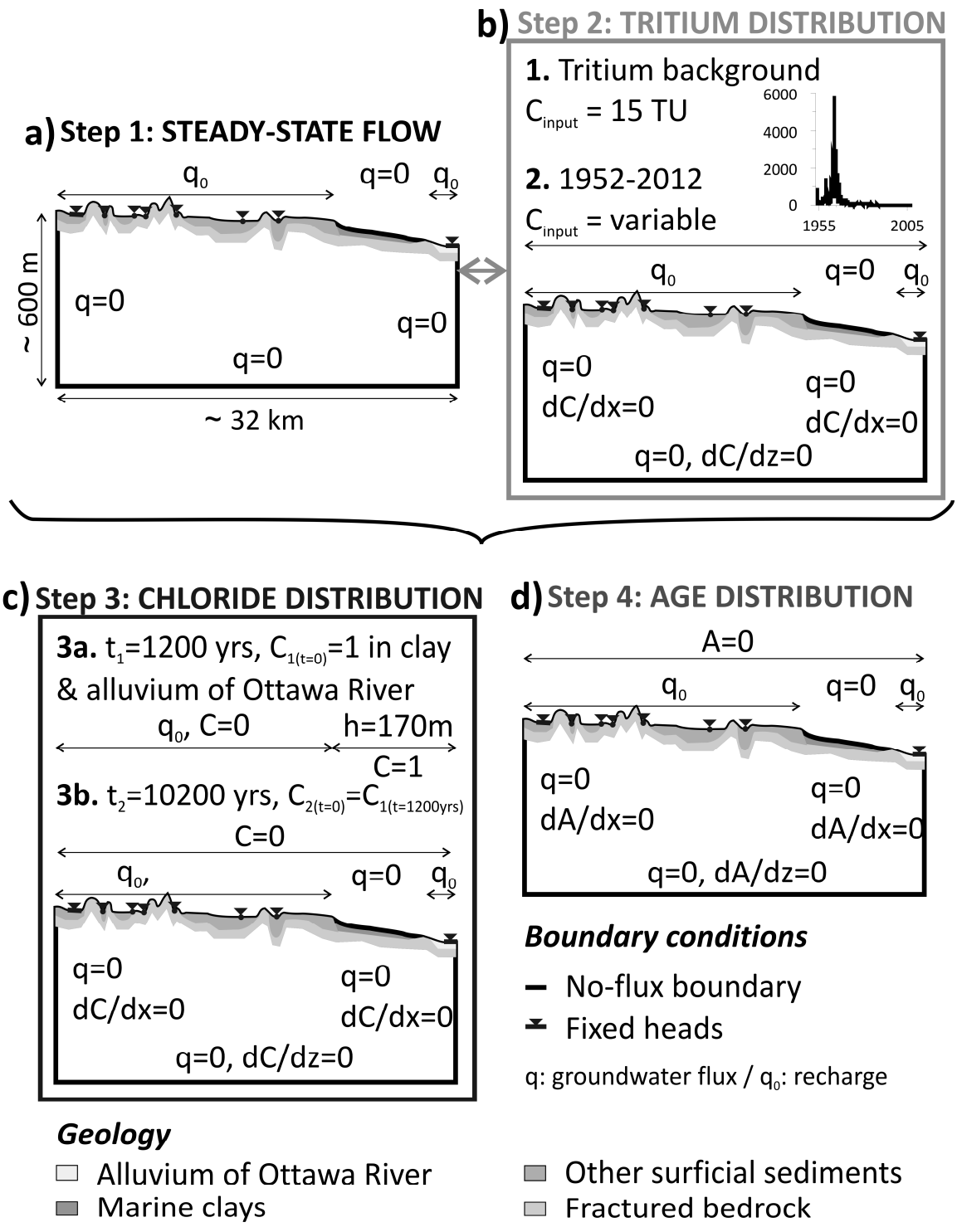
a) Step 1: STEADY-STATE FLOW
q_0
q=0
q_0
~ 600 m
q=0
q=0
q=0
~ 32 km
b) Step 2: TRITIUM DISTRIBUTION
1. Tritium background
C_{input} = 15 TU
6000
4000
2000
0
1955
2005
2. 1952-2012
C_{input} = variable
q_0
q=0
q_0
q=0
dC/dx=0
q=0
dC/dx=0
q=0, dC/dz=0
c) Step 3: CHLORIDE DISTRIBUTION
3a. t_1=1200 yrs, $C_{1(t=0)}$=1 in clay & alluvium of Ottawa River
q_0, C=0
h=170m
C=1
3b. t_2=10200 yrs, $C_{2(t=0)}$=$C_{1(t=1200yrs)}$
C=0
q_0,
q=0
q_0
q=0
dC/dx=0
q=0
dC/dx=0
q=0, dC/dz=0
d) Step 4: AGE DISTRIBUTION
A=0
q_0
q=0
q_0
q=0
dA/dx=0
q=0
dA/dx=0
q=0, dA/dz=0
Boundary conditions
No-flux boundary
Fixed heads
q: groundwater flux / q_0: recharge
Geology
Alluvium of Ottawa River
Marine clays
Other surficial sediments
Fractured bedrock

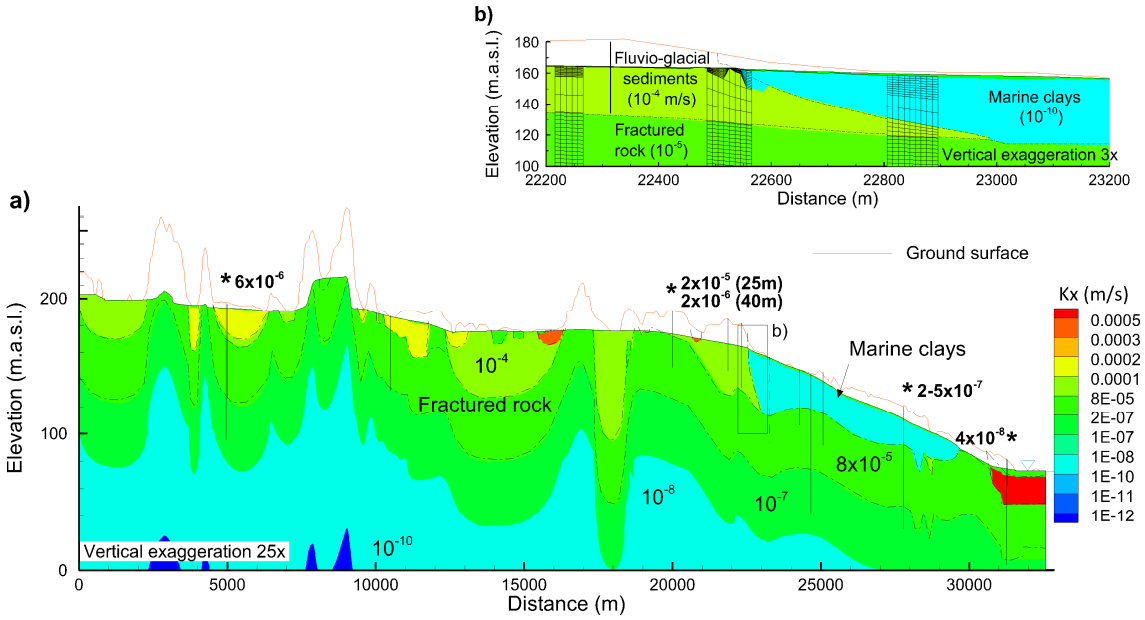
b)
Elevation (m.a.s.l.)
180
160
140
120
100
Fluvio-glacial
sediments
(10-4 m/s)
Fractured
rock (10-5)
Marine clays
(10-10)
Vertical exaggeration 3x
22200
22400
22600
22800
23000
23200
Distance (m)
a)
Elevation (m.a.s.l.)
200
100
0
Ground surface
* 6x10-6
* 2x10-5 (25m)
2x10-6 (40m)
b)
Marine clays
* 2-5x10-7
4x10-8*
10-4
Fractured rock
8x10-5
10-8
10-7
10-10
Vertical exaggeration 25x
Kx (m/s)
0.0005
0.0003
0.0002
0.0001
8E-05
2E-07
1E-07
1E-08
1E-10
1E-11
1E-12
0
5000
10000
15000
20000
25000
30000
Distance (m)

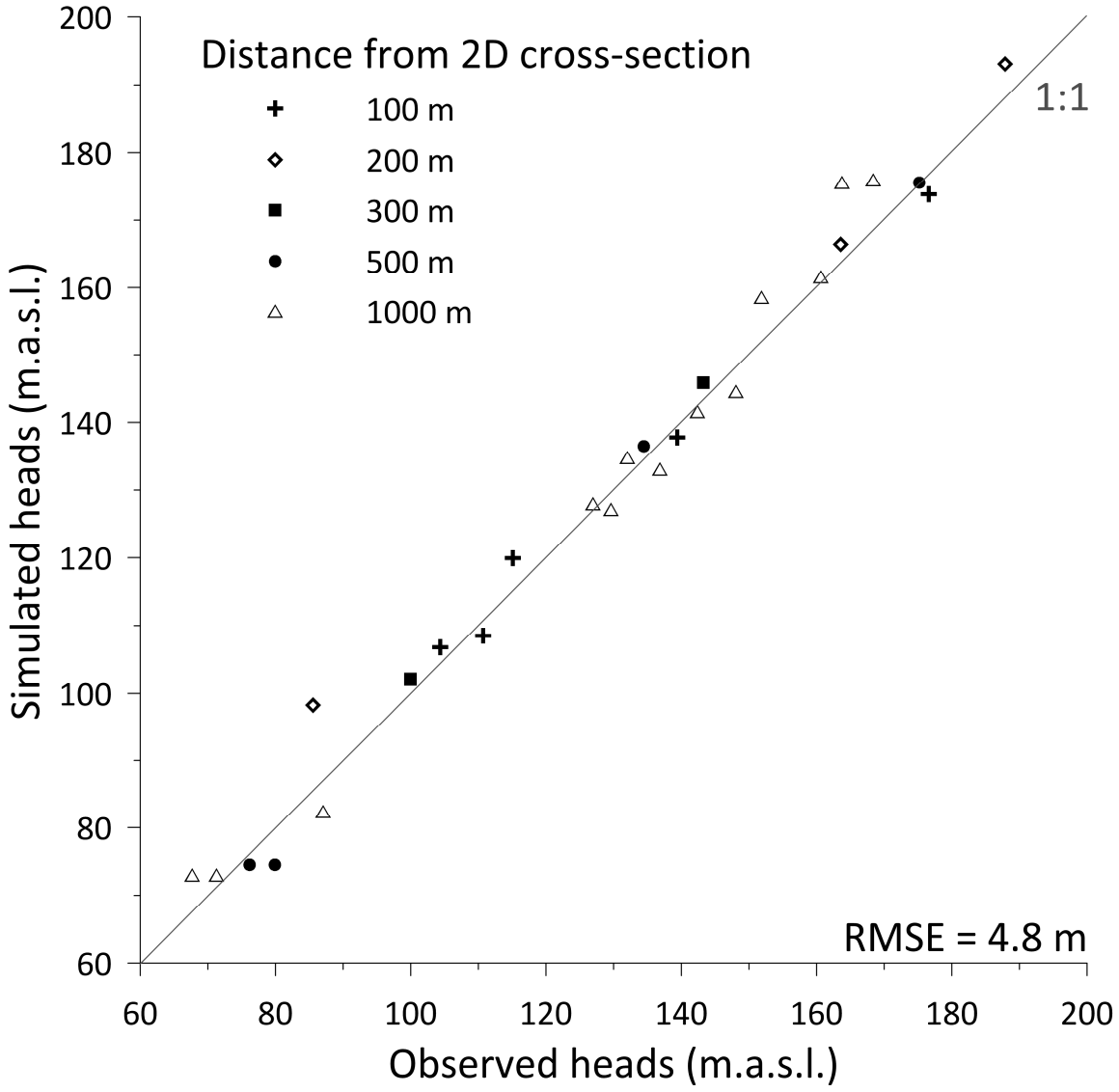
Distance from 2D cross-section
100 m
200 m
300 m
500 m
1000 m
1:1
RMSE = 4.8 m
Simulated heads (m.a.s.l.)
Observed heads (m.a.s.l.)
200
180
160
140
120
100
80
60
60
80
100
120
140
160
180
200

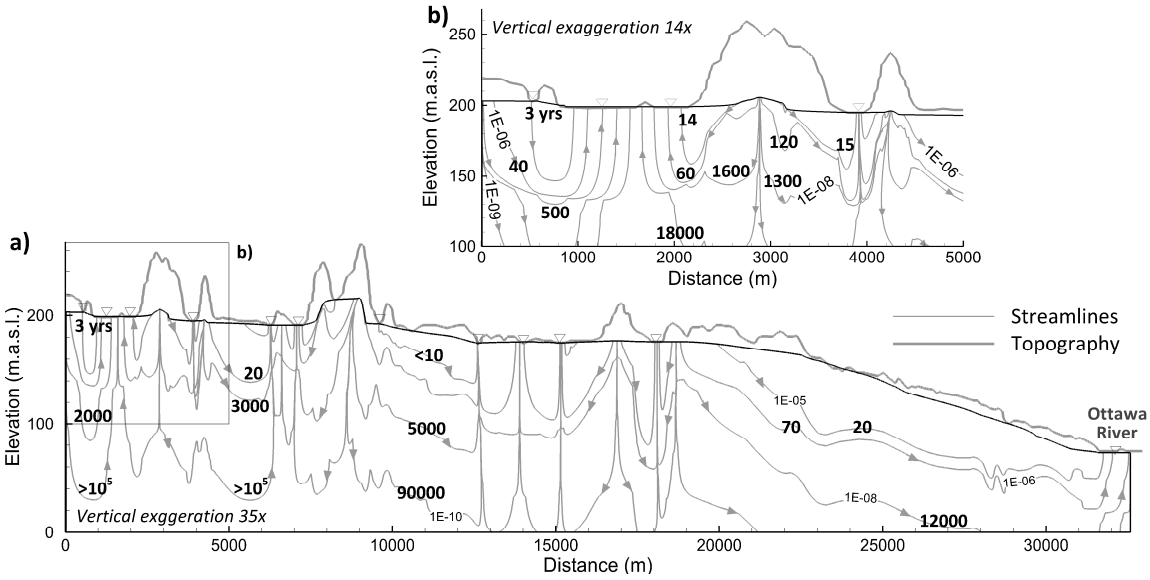
a)
b)
Vertical exaggeration 14x
Elevation (m.a.s.l.)
Distance (m)
3 yrs
14
120
15
40
60
1600
1300
500
18000
1E-06
1E-08
1E-09
Streamlines
Topography
Ottawa River
<10
20
3000
2000
5000
70
90000
12000
>10^5
Vertical exggeration 35x

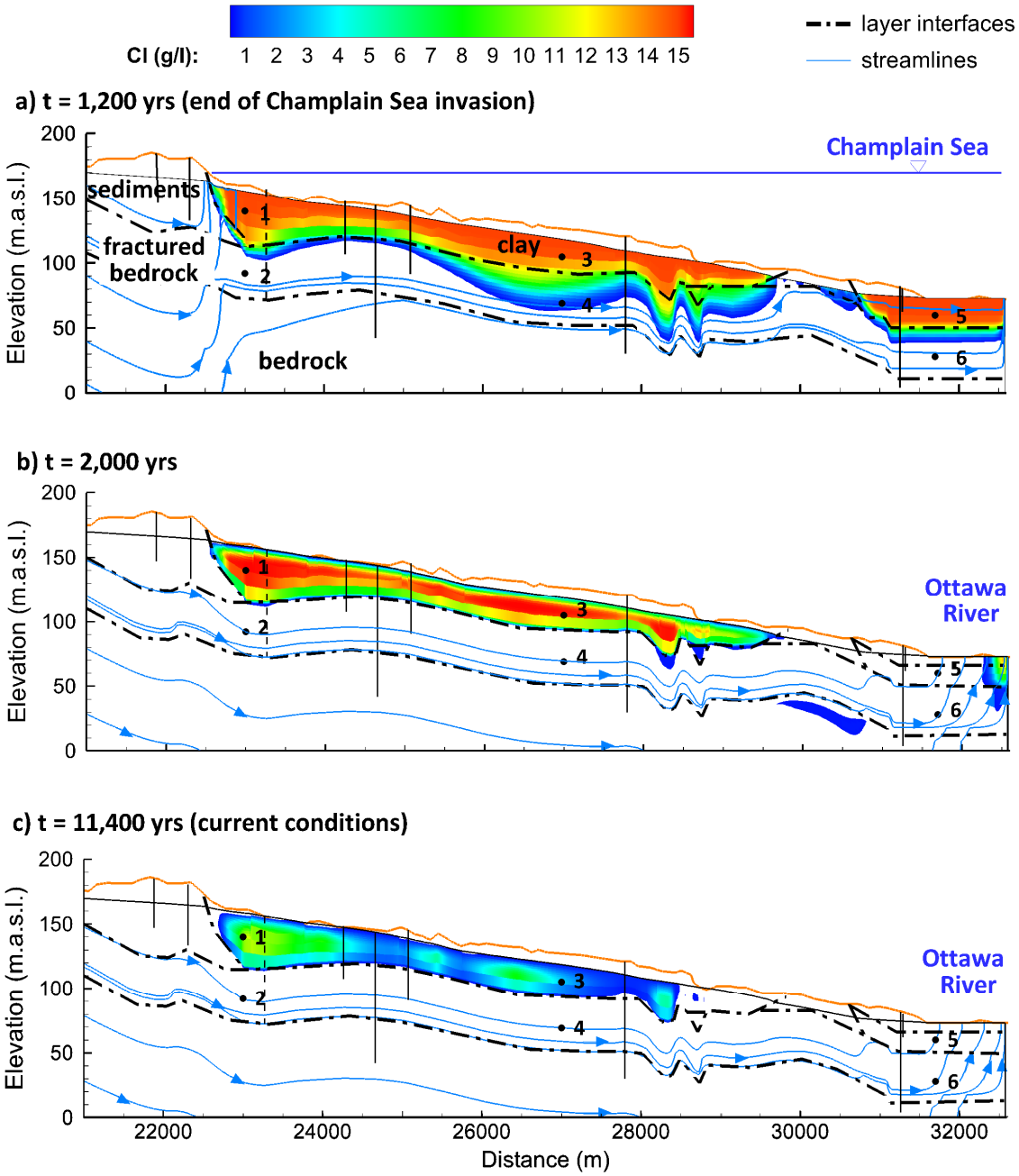
Cl (g/l): 1 2 3 4 5 6 7 8 9 10 11 12 13 14 15
layer interfaces
streamlines
a) t = 1,200 yrs (end of Champlain Sea invasion)
Champlain Sea
sediments
fractured bedrock
clay
bedrock
Elevation (m.a.s.l.)
b) t = 2,000 yrs
Ottawa River
c) t = 11,400 yrs (current conditions)
Ottawa River
Distance (m)

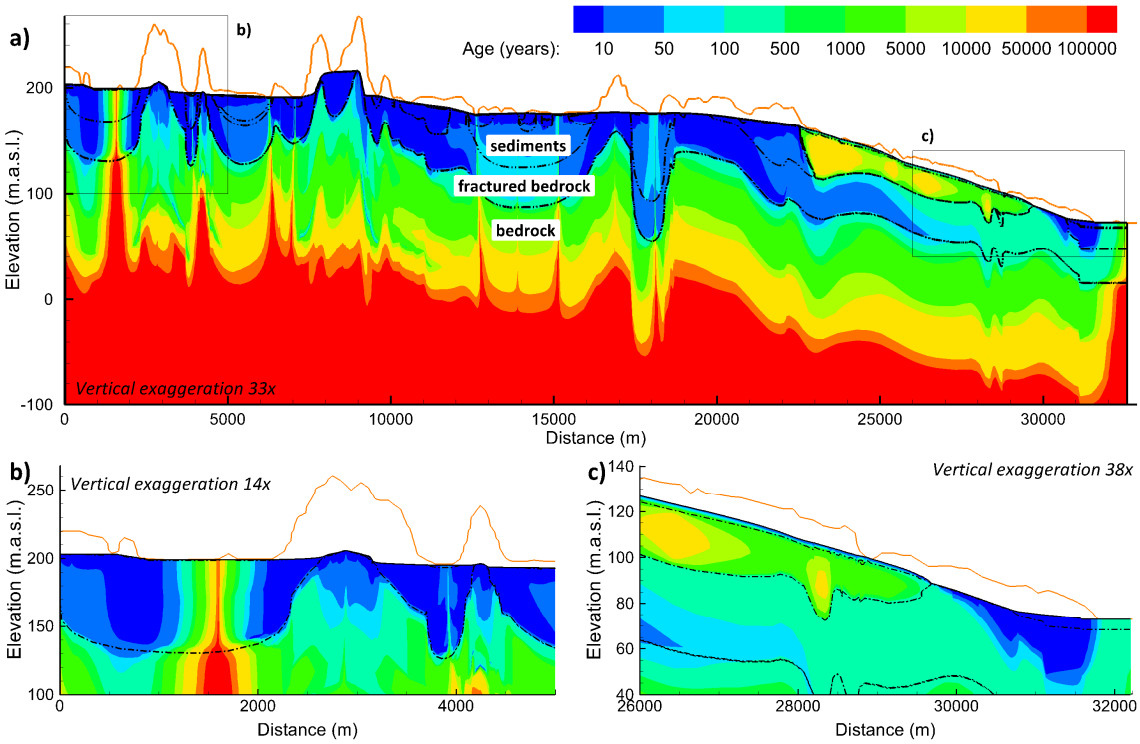
a)
b)
c)
Age (years):
10
50
100
500
1000
5000
10000
50000
100000
sediments
fractured bedrock
bedrock
Vertical exaggeration 33x
Elevation (m.a.s.l.)
Distance (m)
Vertical exaggeration 14x
Vertical exaggeration 38x

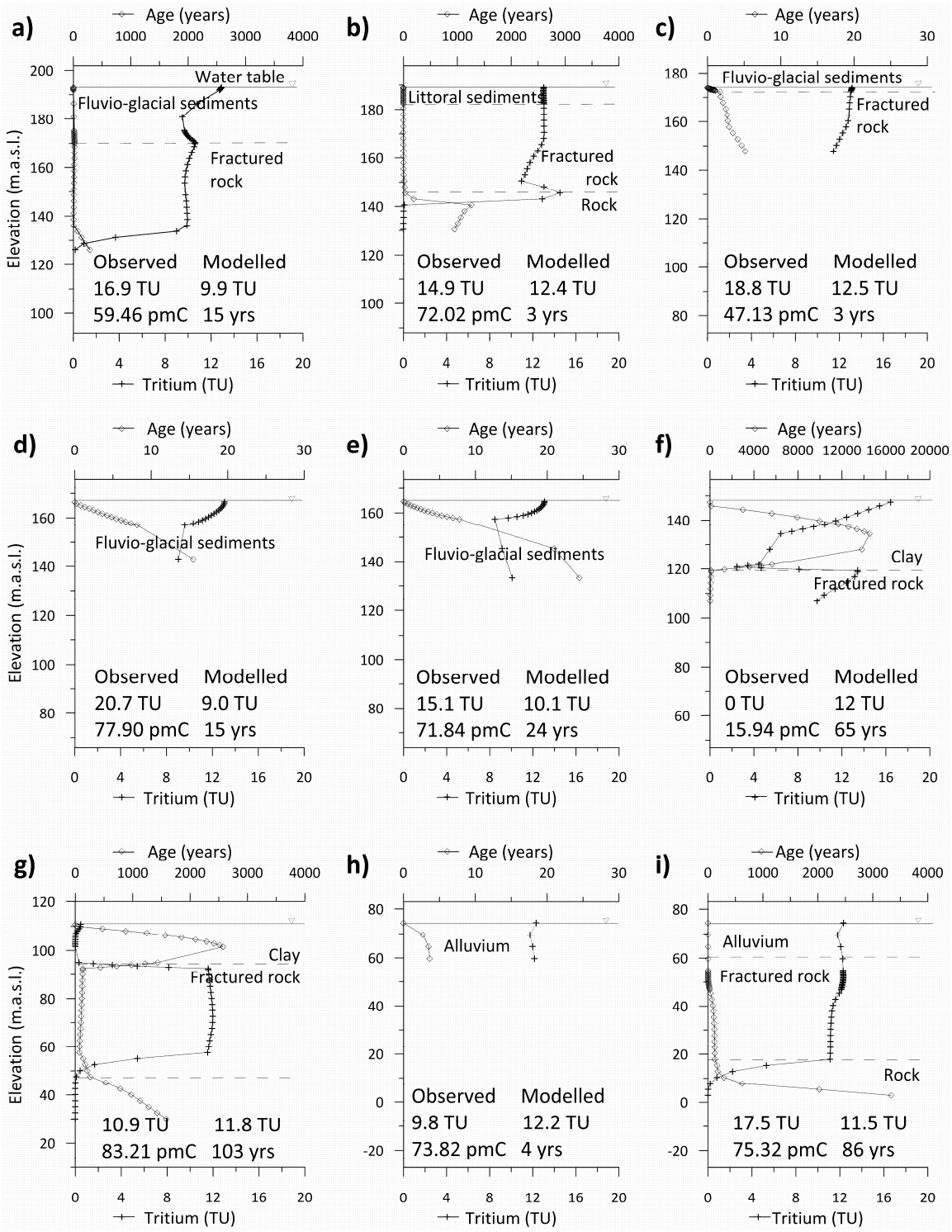
a)
Age (years)
Water table
Fluvio-glacial sediments
Fractured rock
Observed Modelled
16.9 TU 9.9 TU
59.46 pmC 15 yrs
Elevation (m.a.s.l.)
Tritium (TU)
b)
Littoral sediments
Fractured rock
Rock
Observed Modelled
14.9 TU 12.4 TU
72.02 pmC 3 yrs
c)
Fluvio-glacial sediments
Fractured rock
Observed Modelled
18.8 TU 12.5 TU
47.13 pmC 3 yrs
d)
Fluvio-glacial sediments
Observed Modelled
20.7 TU 9.0 TU
77.90 pmC 15 yrs
e)
Fluvio-glacial sediments
Observed Modelled
15.1 TU 10.1 TU
71.84 pmC 24 yrs
f)
Clay
Fractured rock
Observed Modelled
0 TU 12 TU
15.94 pmC 65 yrs
g)
Clay
Fractured rock
10.9 TU 11.8 TU
83.21 pmC 103 yrs
h)
Alluvium
Observed Modelled
9.8 TU 12.2 TU
73.82 pmC 4 yrs
i)
Alluvium
Fractured rock
Rock
17.5 TU 11.5 TU
75.32 pmC 86 yrs

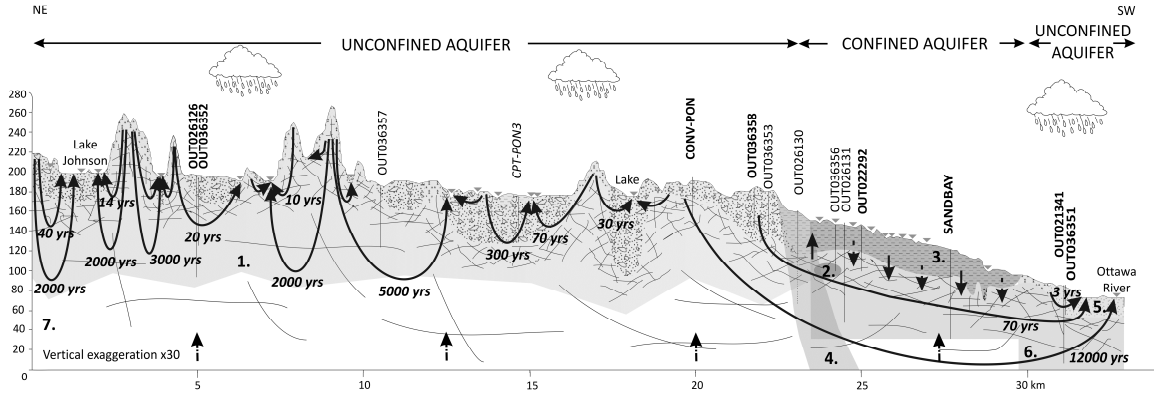

LEGEND

Geology

Quaternary deposits

- Alluvial deposits (sand)
- Sand & gravel
- Marine clay
- Till
- Surface water

Bedrock

- Fractured Canadian Shield

Fluxes

- Groundwater flow
- Diffusive flux of NaCl
- Diffusive flux of ^4He

Well identification

Well ID: well on the flow line

Well ID: well a bit offset from the flow line

Well ID: well offset from the flow line (chemistry considered as representative of the geologic unit)

Geochemical zones

1. $Ca\text{-}HCO_3$ water type
Increase of Ca^{2+}, HCO_3^- and TDS concentrations along the flow path (silicate weathering)

Na-Cl water type

2. Remnant Champlain Sea water (stagnant zone)

3. Probably mixed with $Ca\text{-}HCO_3$ water type at the top of the clay layer ($Na\text{-}HCO_3$)

4. Transition zone

5. $Ca\text{-}HCO_3$ water type
Discharge zone characterised by mixing with $Na\text{-}HCO_3$ water type

6. $Na\text{-}HCO_3$ water type
Na^+/Ca^{2+} cation exchange (Na-Cl water type flushed away by $Ca\text{-}HCO_3$ water type)

7. No available chemical data
Most likely $Ca\text{-}HCO_3$ and $Na\text{-}HCO_3$ up and down-gradient of the transition zone

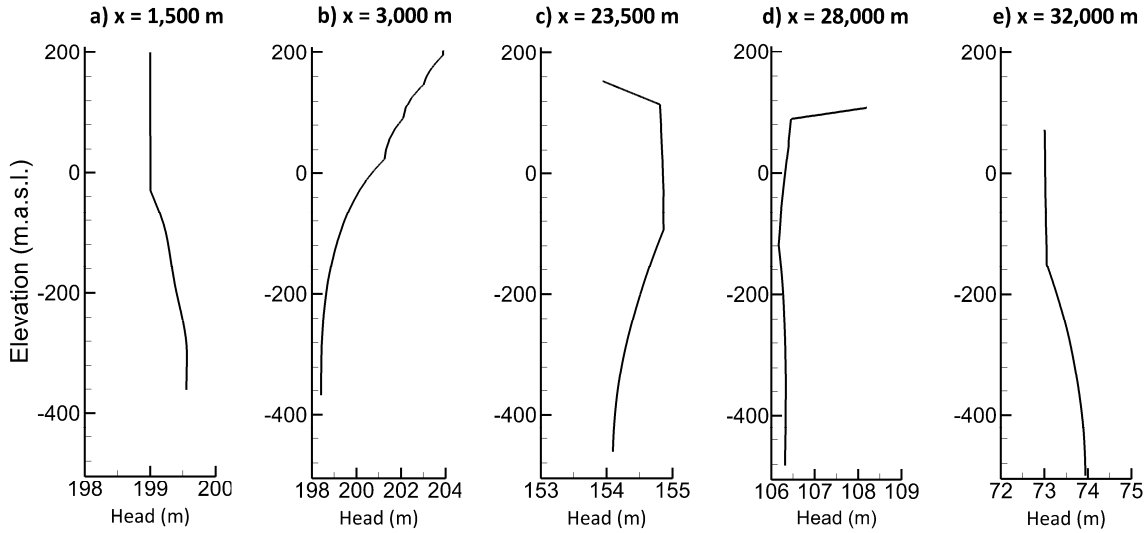
a) x = 1,500 m
b) x = 3,000 m
c) x = 23,500 m
d) x = 28,000 m
e) x = 32,000 m
Elevation (m.a.s.l.)
Head (m)

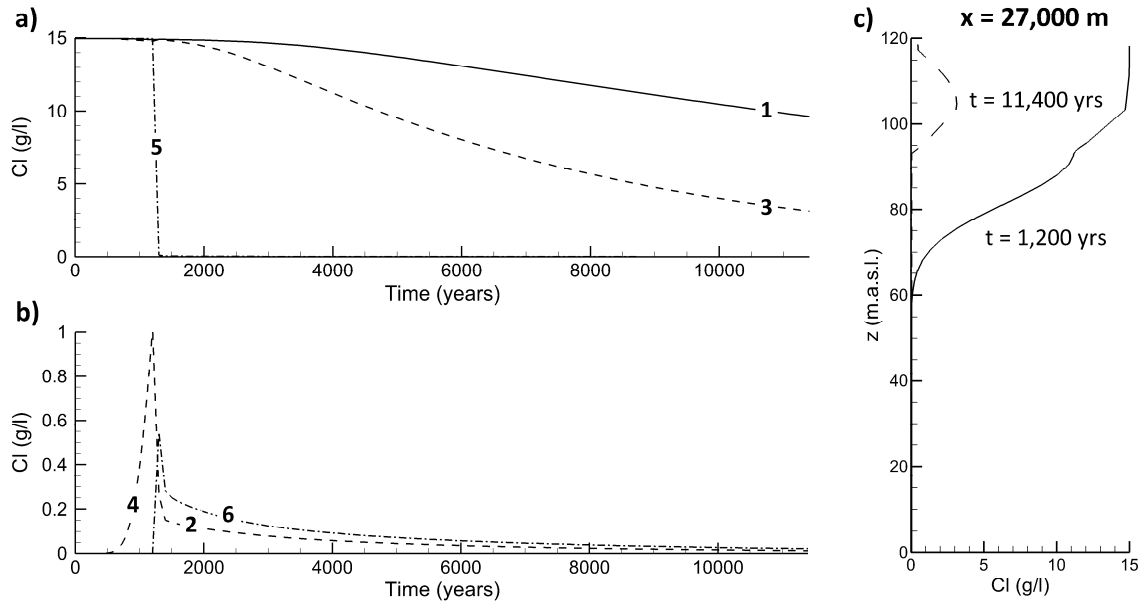
a)
Cl (g/l)
Time (years)
1
3
5
b)
Cl (g/l)
Time (years)
2
4
6
c)
x = 27,000 m
t = 11,400 yrs
t = 1,200 yrs
z (m.a.s.l.)
Cl (g/l)

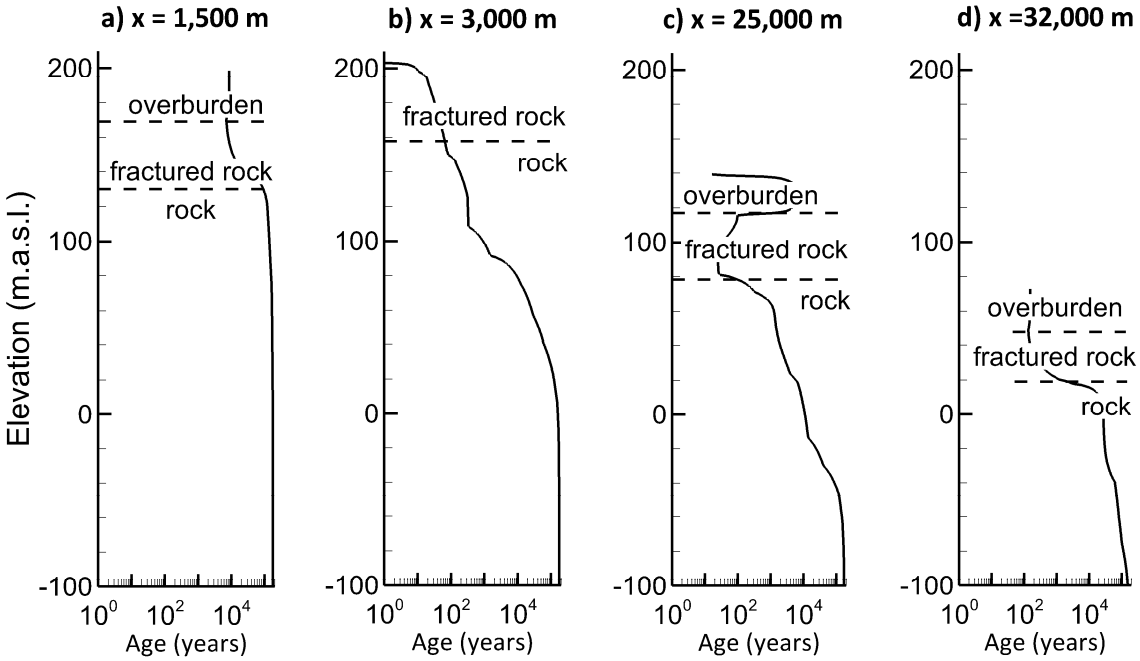
a) x = 1,500 m
b) x = 3,000 m
c) x = 25,000 m
d) x =32,000 m
Elevation (m.a.s.l.)
200
100
0
-100
overburden
fractured rock
rock
10^0 10^2 10^4
Age (years)